



INSTITUTO SUPERIOR TÉCNICO
Universidade Técnica de Lisboa

Dynamics and Control of a High Speed Train Pantograph System

Tiago Manuel Oliveira Valezim Teixeira

Dissertação para obtenção do Grau de Mestre em
Engenharia Mecânica

Júri

Presidente:	Professor José Manuel Gutierrez Sá da Costa
Orientador:	Professor José Manuel Gutierrez Sá da Costa
Co-Orientador:	Professor Jorge Manuel Mateus Martins
Vogal:	Professor Miguel Afonso Dias de Ayala Botto

Setembro - 2007

Este trabalho reflecte as ideias dos seus
autores que, eventualmente, poderão não
coincidir com as do Instituto Superior Técnico.

Abstract

High speed trains permit faster travelling between long distance destinations, making it an easy and comfortable way of travelling. The pantograph is the element of the train that collects electrical current from the cable system above (the catenary), to the train motors. The contact force variation can cause contact losses, electric arc formations and sparking. This deteriorates the quality of current collection and increases the electrical related wear, therefor becoming a limiting factor for the maximum train speed. The increase of the static contact force is not an efficient way to deal with the problem, because it increases mechanical abrasive wear and produces an excessive uplift of the contact wire. Maintaining the contact force in an admissible region is crucial for high speed trains. In this work a model in *SimMechanics*[®] is created for the pantograph and the catenary; the complexity of the contact interface between the pantograph and the catenary is studied. The control strategy is based on a *PID* controller, and robust H_2 and H_∞ controllers. Both approaches are studied and compared. A virtual reality pantograph is created for better perception of the motion of the pantograph. The main targeted conclusion is to confirm that the usage of robust control is superior and more flexible than classical *PID* control strategies making the current collection constant, and therefore producing low wear of the registration strip. Furthermore, we verify that model approximations are very influent on contact force dynamics.

Keywords: Pantograph, Catenary, Robust controller, Modelling, Closed chain systems.

Resumo

Os comboios de alta velocidade permitem viajar de forma rápida a longas distâncias, de forma fácil e confortável. O pantógrafo é o elemento do comboio que recolhe a corrente eléctrica do sistema de cabos acima (a catenária), distribuindo-a aos motores do comboio. A variação da força pode causar perdas de contacto, formando arcos eléctricos. Com a deterioração da qualidade da colecta de corrente há um aumento do desgaste relacionado com arcos eléctricos, transformando-se num factor limitativo para o comboio atingir velocidades elevadas. O aumento da força estática de contacto não é uma forma eficaz de tratar o problema, porque aumenta o desgaste abrasivo mecânico entre o pantógrafo e o cabo da catenária. Manter a força de contacto numa região admissível é crucial para comboios de alta velocidade. Neste trabalho é criado um modelo em *SimMechanics*[®] para o pantógrafo e a catenária; a complexidade do interface de contacto entre o pantógrafo e a catenária será estudada. A estratégia de controlo será baseada num controlador *PID*, e num controlador robusto H_2 e H_∞ , ambas as abordagens serão estudadas e comparadas. Será criado um pantógrafo em realidade virtual para melhor percepção do seu movimento. A principal conclusão alvejada é confirmar que o uso de controlo robusto, é superior e mais flexível a estratégias de controlo do tipo *PID*, fazendo com que a colecta de corrente eléctrica seja constante, diminuindo o desgaste no pantógrafo. Também é verificado que as aproximações definidas no modelo criado são muito influentes nos valores da força de contacto e comportamento do sistema.

Palavras chave: Pantógrafo, Catenária, Controlador Robusto, Modelação, Sistema em árvore fechado.

Acknowledgments

I would like to make a special thanks to Professor José Manuel Gutierrez Sá da Costa and Professor Jorge Manuel Mateus Martins for the time spent in the project. I am very grateful to Professor Rui Loureiro for giving important information relative to railway norms including pantographs and for setting up a study visit to the Fertagus repair station. I am also very grateful to Eng. Victor Gonçalves for all the help and information given in the study visit.

Index

1	Introduction	1
1.1	Pantograph systems	3
1.2	Objectives	4
1.3	Contributions of this thesis	5
1.4	Thesis Outline	5
2	Basic rail system concepts	7
2.1	Power supply	7
2.1.1	AC or DC traction	8
2.2	The catenary	8
2.2.1	Catenary suspension systems	10
2.3	The pantograph	10
2.3.1	Standard speed trains	11
2.3.2	High speed trains	12
2.3.3	Force control pantograph on high speed train	12
2.4	Passive pantograph limitations	13

3	Dynamics modelling in SimMechanics®	15
3.1	SimMechanics®	15
3.2	Modelling multibody systems	16
3.3	Relative versus absolute coordinate formulations	16
3.4	Unconstrained systems	17
3.5	Analysis of simple chain systems	17
3.6	Linearization	22
4	SimMechanics® pantograph model	25
4.1	Pantograph body elements	26
4.1.1	Basic components	26
4.1.2	Passive elements	26
4.1.3	Active elements	28
4.1.4	Joints	29
4.2	Physical modelling blocks	29
4.3	Major Steps of the Dynamical Analysis	30
4.4	Creating a Pantograph in SimMechanics®	31
4.4.1	Initial configurations	31
4.4.2	Linking the data file to the SimMechanics® model	32
4.4.3	SimMechanics® pantograph model	33
4.4.4	The catenary model	34
4.5	Pantograph models	35

<i>INDEX</i>	ix
4.6 Linearization and Trimming in SimMechanics [®]	37
4.7 Visualization Tools	38
4.8 Virtual model and world creation	38
4.9 SimMechanics [®] VRML model integration	39
5 Pantograph control	41
5.1 Introduction to robust controllers	42
5.1.1 Robust control preliminaries	42
5.1.2 The sensitivity function	45
5.1.3 The complementary sensitivity function	47
5.1.4 The trade-off	48
5.1.5 Weighted sensitivity	48
5.1.6 Summary	49
5.2 H_2 and H_∞ optimal control	50
5.2.1 H_2 optimal control	51
5.2.2 H_∞ optimal control	52
5.2.3 Robustness	52
5.3 Pantograph control implementation	52
6 Results and discussion	55
6.1 Pantograph type overview	55
6.2 Pantograph type overview	56
6.3 Linearization	58

6.3.1	Linearization of the nonlinear model	59
6.3.2	Conclusions from linearization	62
6.4	Problem statement	63
6.5	Experimental results and motivation	64
6.6	Pantograph and catenary nonlinear model attributes	67
6.6.1	Conclusions from open-loop modelling	69
6.6.2	Model comparison with experimental results	71
6.7	Model sensitivity to parameter changes	71
6.8	Closed-loop pantograph analysis	73
6.8.1	Controller development	74
6.8.2	Results	79
6.9	Mixed control analysis	85
6.10	Sliding catenary control	87
6.11	Controller robustness to model changes	88
7	Conclusions and future work	91
7.1	Future work	93
	Bibliography	94

Figure Index

1.1	Model and Control diagram	3
2.1	Catenary system	9
2.2	Catenary	10
2.3	Pantograph and train	11
2.4	<i>Faiveley</i> pantograph CX	12
2.5	Pantograph calibration	13
3.1	Bodies and joints in a serial chain	21
3.2	Plant to linearize	23
4.1	The pantograph	25
4.2	Pantograph elements	28
4.3	Passive elements	28
4.4	Joint positioning	29
4.5	Joints (SimMechanics [®] representation)	30
4.6	SimMechanics: Parameters	31
4.7	Data model	32

4.8	Generic mass data	33
4.9	Mass orientation	33
4.10	Equivalent model of the Catenary	34
4.11	Catenary representation	35
4.12	Linearization process for control	36
4.13	Pantograph configurations studied	36
4.14	VRML model	39
4.15	Linking SimMechanics with VR Sink	39
4.16	SimMechanics model connection to VRML model	40
5.1	Simple control loop system with uncertainty	43
5.2	Schematic of conventional feedback control loop	45
5.3	Sensitivity and Complementary Sensitivity functions of a closed-loop with a PI controller and a 1st-order system without delay	50
5.4	Weight functions	51
5.5	Pantograph control closed loop representation	53
6.1	Pantograph with one actuator and with springs and dampers present in the registration strip (Type 1)	55
6.2	One actuator pantograph with fixed registration strip (Type 2)	57
6.3	One actuator pantograph with 2 <i>DOF</i> registration strip (Type 3)	57
6.4	The Type 4 and Type 5 pantograph models	58
6.5	Model validation: input variation	60

6.6 Pole Zero Map: Torque in joint vs Force in catenary (G_1)	61
6.7 Pantograph linear models	63
6.8 Training Session in High Speed Systems	65
6.9 <i>SNCF</i> experimental results	66
6.10 Free body diagram of Type 1 registration strip	67
6.11 Pantograph model representation	68
6.12 Pantograph open-loop with catenary step perturbation	69
6.13 Pantograph open-loop with catenary sine perturbation	70
6.14 Type 1, 2Hz, with 10 cm amplitude, sinusoidal catenary perturbation	71
6.15 Type 3, 2Hz, with 10 cm amplitude, sinusoidal catenary perturbation	72
6.16 Model mass parameter and pole-zero map	72
6.17 Model spring parameter and pole-zero map	73
6.18 Model damper parameter pole-zero map	74
6.19 Testing w_1 : Loop shaping	76
6.20 Multiple models based on Type 1 model	76
6.21 Robust Controller gain plot	78
6.22 Type 1 with 2Hz sine perturbation controller comparisons	79
6.23 Type 1 step perturbation controller comparisons	79
6.24 Type 1 with 20Hz sine perturbation controller comparisons	80
6.25 Type 1 step perturbation with new controller	81
6.26 Type 1 with 20Hz sine perturbation and new controller	81

6.27 Type 3 with $2Hz$ sine perturbation with new controller	83
6.28 Type 3 with $20Hz$ sine perturbation and new controller	83
6.29 H_∞ controller, with no damper in lower joint	85
6.30 Type 4 controller implementation results to sine perturbation	86
6.31 Type 4 controller implementation results to step perturbation	86
6.32 Independent control function of Type 5 model	87
6.33 Type 5 control implementation for $2Hz$ perturbation	88
6.34 H_∞ VS PID controlled with altered model (no lower damper)	89
6.35 Noise influence on Type 1 model with $2Hz$ catenary influence	90

Table Index

4.1	Rigid body mass and inertia	27
4.2	Rigid body initial position and orientation	27
4.3	Passive elements information	29
4.4	Pantograph model type considerations	37
6.1	Poles and Zeros	61
6.2	Global <i>SNCF</i> pantograph experimental results	66
6.3	Experimental results highlights	66

Abbreviations

AC	Alternate current
DC	Continuous current
PID	Proportional Integrative Derivative
PD	Proportional Derivative
CT	Continuous Time
LTI	Linear Time Invariant
k	Stiffness coefficient
l	Natural length
c	Damping coefficient
RNE	Recursive Newton Euler
CM	Center of mass
ODE	Ordinary differential equations
PDE	Partial differential equations
VRML	Virtual Reality Modelling Language
CX	SNCF high speed pantograph model
SNCF	Railway company in France

Chapter 1

Introduction

High speed rail vehicles are a comfortable and fast way of transportation. Until today open loop pantograph systems proved to be a very robust solution for trains. Because of rail line degradation, train circulation with adverse weather conditions, like intense wind, and the desire to achieve higher speeds, can cause excessive wear in the pantograph contact interface. Improving high speed circulation on the railway isn't the only goal in the present study, low cost maintenance of the pantograph and the catenary is equally important, thus the ideal solution would be of having a system that has low maintenance comparing with present solutions, higher train circulation speeds and to avoid the necessity of changing the whole railway system, including the catenary. Train speed, and pantograph actuating force with the catenary, are the primary variables to maintain a stable current collection.

High speeds generally produce lower contact forces. A problem that arises from building faster trains is in the current collector of the train, the pantograph. In order to collect electric current from the cable network system above the train, the catenary, it is necessary for the pantograph to contact the catenary. Excessive contact force causes damage to the pantograph and the lack of contact force causes current perturbation and electric arcs which damages the pantograph.

Maintaining the contact force in an admissible region is very important, in order to achieve sustainable high speeds. Comparing to standard open loop systems, closed loop systems allow train circulation speed to up to 500 Km/h and more depending on other limiting factors (not the pantograph interface but to other train related variables).

There is a wide variety of electric traction systems around the world, which have been built according to the type of railway, its location and the technology available at the time of the installation. Many installations seen today were first built up to 100 years ago, when electric traction was barely out, and this has had a great influence on what is seen today.

However, in the last 20 years there has been a gigantic acceleration in railway traction development. This has run in parallel with the development of power electronics and microprocessors. What have been the accepted norms for the industry for, 80 years, have suddenly been thrown out and replaced by fundamental changes in design, manufacture and operation. The result has been top speed circulation of 500 Km/h.

The *SNCF* train pantograph functions as follows: it is activated by a pneumatic device comprised of an air cushion controlled by an electro-pneumatic plate and assisted by an electronic board. The system adjusts the air cushion pressure, and at the same time, the force to apply on the catenary, in real time, to obtain the best possible electrical contact between the catenary and the pantograph, regardless of operating conditions. The applied pressure is calculated according to the speed of the train-set, taking the load bearing capacity of the pantograph itself, the movement direction and the composition of the train-set (single unit or multiple unit) into account.

In order to have active control in the pantograph, it is necessary to know the dynamic nonlinear model of a real pantograph. In this work we consider the *CX* pantograph model of the *SNCF* trains.

The catenary will be modelled as a parallel spring / damper system connected to the registration strip of the pantograph, this element has direct contact with the catenary. After obtaining the nonlinear model, a virtual reality model will be created in order to visualize the motion of the pantograph. The control strategies will be applied to the nonlinear model in order to get the contact force in an admissible region of tolerance. Three controllers will be studied: *PID* controller, robust H_2 and H_∞ controllers. The robust controllers will require a linear model of the system which will be obtained by linearizing the nonlinear model around the nominal conditions. Figure 1.1 shows a view of the integrated modelling and control process, an example of this approach can be seen in [1].

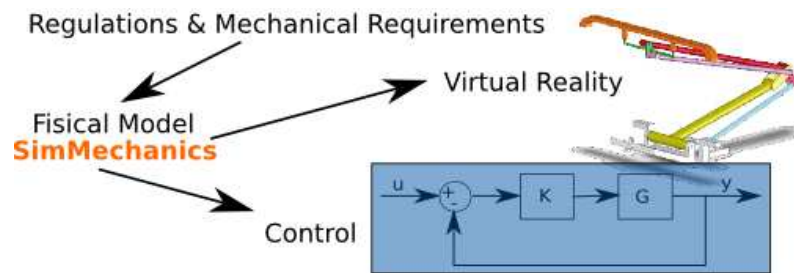


Figure 1.1: Model and Control diagram

Figure 1.1 illustrates the process of creation of the closed loop system presented in this work. A model has to be created, which contains all the information of a real pantograph. After the model has been created, a closed loop feedback system has to be developed. Using the model created (represented in the figure as G) and a controller K that has to be tuned. The motion of the pantograph is visualized in a virtual reality world.

1.1 Pantograph systems

Much investigation has been done around turning the railway system faster and safer. In order for the train to work, current collection has to be done and thus the usage of a catenary to deliver current from the energy power plant, and the pantograph to collect current towards the train engines. These

1.2 Objectives

systems act together as one but research was done separately until today.

Modeling a pantograph and catenary system was one of the main objectives in the past to correctly simulate a high speed train. Many authors studied this with sensitivity analysis [2] which finds relations in model variables and performance of a catenary - pantograph system, they also modelled the catenary with a *FEM* (finite element method) based approach. A more extended approach has been used in [3], [4] and [5], a model was developed and studied but in a more explicit way. The catenary elements and derivation are farther developed. The effect of locomotive vibration on pantograph is treated in [6]. A pantograph system isn't just about modelling, new advances have been made in robust controlling of pantograph systems and some interesting results are presented in [7], [8] and [9]. The controllers implemented in these papers range from simple *PID* controllers to more complex theories like robust controllers. All citations made until now are essential to the problem layout and solution search, but although the results look interesting the implementation is fairly complicated, the best approach found can be seen in [1]. In this paper a engineering point of view in robust controller tuning was used, recurring to simple sinusoidal perturbation functions.

1.2 Objectives

The main goal of this study is to model and control the *CX* pantograph to maintain the contact force in a admissible region; to study the best control configuration and control strategy. Two control strategies will be studied: a *PID* controller which is a standard control method and an advanced controller based on the robust control theory H_2 and H_∞ .

1.3 Contributions of this thesis

To simplify the modelling process, instead of using classical formulations to obtain numerical results, *SimMechanics*[®] was used. To *simMechanics*[®] a pantograph is a multibody closed mechanical system and thus the theory presented in [10] and [11] where useful in the model creation.

The primary software used is *Matlab*[®] / *Simulink*[®] with its mechanical modelling environment called *SimMechanics*[®]. This environment is built upon the basic concepts of general mechanical systems, details can be seen in [12]. Many new researchers are starting to use *Matlab*'s powerful modelling environment for system analysis, and some research has been done in this area [13].

This project brings a pantograph model constructed upon *SimMechanics*[®], with a robust controller attached to the target joints (will be studied in the next chapters). Not only is it important to model and control a pantograph, but to understand the limitations and advantages of the combination of many *Matlab*[®] toolbox tools. Another contribution of this theses is the use of many *Matlab* tools applied to robust control of a pantograph, like the usage of the *Robust Control Toolbox*.

1.4 Thesis Outline

In chapter 1, an introduction to all work developed is made. In chapter 2, basic railway definitions are introduced. In chapter 3, it is explained how *SimMechanics*[®] formulates the dynamic equations solved numerically. In chapter 4: various pantograph model and catenary elements are developed and explained their *SimMechanics*[®] implementation. In chapter 5, the control theory used to project the closed loop controller is presented. In chapter 6, results are presented and discussed. In chapter 7, conclusions and future work are presented.

Chapter 2

Basic rail system concepts

2.1 Power supply

The electric railway needs a power supply that the trains can access at all times. It must be safe, economical and easy to maintain. It can use either direct current (DC) or alternating current (AC). The former has been for many years, simpler for railway traction purposes. The latter is better over long distances and cheaper to install however, it has been until recently, it has been more complicated to control at train level.

Transmission of power is always performed along the track by means of an overhead wire or at ground level, using an extra third rail laid close to the running rails. AC systems always use overhead wires, DC can use either an overhead wire or a third rail, both are common. Both overhead systems require at least one collector attached to the train so it can always be in contact with the power cable. Overhead current collectors use a "pantograph", so called because that was the shape of most of them until about 30 years ago. The return circuit is via the running rails back to the substation. The running rails are at earth potential and are connected to the substation.

2.2 The catenary

2.1.1 AC or DC traction

It doesn't really matter whether we have AC or DC motors, nowadays either can work with an AC or DC supply. The only requirement is to have the right sort of power electronics between the supply and the motor. However, the choice of AC or DC power transmission system along the line is important. Generally, it's a question of what sort of railway is available. It can be summarized simply as AC for long distance and DC for short distance.

It is easier to boost the voltage of AC than that of DC, so it is easier to send more power over transmission lines with AC. As AC is easier to transmit over long distances, it is an ideal medium for electric railways. DC, on the other hand, is the preferred option for shorter lines: urban systems and tramways. However, it is also used on a small number of main line railway systems.

2.2 The catenary

The mechanics of power supply wiring is not as simple as it may seem. Hanging a wire over the track, providing it with current and running trains under it is not that easy if it is to do the job properly and last long enough to justify the expense of installing it. The wire must be able to carry the current (several thousand amps), remain in line with the route, withstand wind, extreme cold and heat and other hostile weather conditions.

Overhead catenary systems, called "catenary" due to the curve formed by the supporting cable (fig. 2.1), have a complex geometry, nowadays usually designed by computer. The contact wire has to be held in tension horizontally and pulled laterally to negotiate curves in the track. The contact wire tension is typically in the region of 2 tonnes. The wire length is usually between 1000 and 1500 meters, depending on the temperature ranges. The wire is zigzagged relative to the center line of the

track to even the wear on the trains registration strip as it runs underneath (fig. 2.2b).

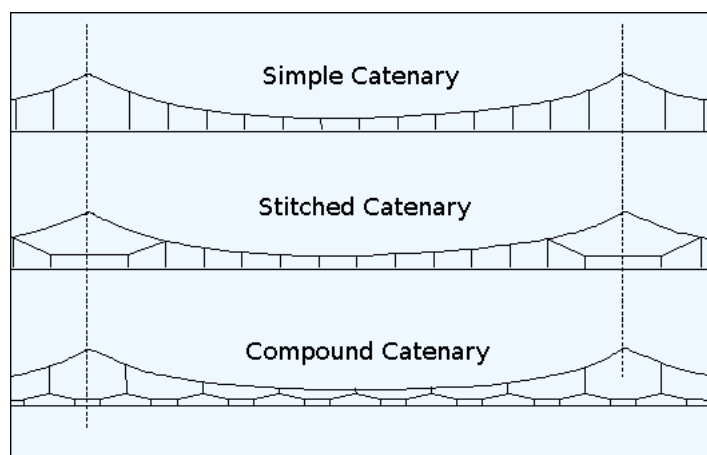


Figure 2.1: Catenary system

The contact wire is grooved to allow a clip to be fixed on the top side. The clip is used to attach the dropper wire. The tension of the wire is maintained by weights suspended at each end of its length. Each length is overlapped by its neighbor to ensure a smooth passage for the registration strip. Incorrect tension, combined with the wrong speed of a train, will cause the pantograph head to start bouncing. An electric arc occurs with each bounce, the registration strip and wire will both become worn through under such conditions.

More than one pantograph on a train can cause a similar problem when the leading pantograph head sets up a wave in the wire and the rear head can't stay in contact. High speeds worsen the problem. The French *TGV* (High Speed Train) formation has a power car at each end of the train but only runs with one pantograph raised under the high speed 25 *kV* AC lines. The rear car is supplied through a 25 *kV* cable running the length of the train. This is prohibited in Britain due to the inflexible safety approach there.

A waving wire will cause another problem. It can cause the dropper wires, from which the contact wire is hung, to “kink” and form little loops. The contact wire then becomes too high and decreases

2.3 The pantograph

contact.

2.2.1 Catenary suspension systems

Various forms of catenary suspension are used (fig. 2.1). Catenary information may be found in [14] for example, and depends on the system, its age, its location and the speed of trains using it. Broadly speaking, the higher the speeds, the more complex the “stitching“, although a simple catenary will usually suffice if the support posts are close enough together on a high speed route. Modern installations often use the simple catenary, slightly sagged to provide a good contact. It has been found to perform well at speeds up to 200 km/h. Figure 2.2a shows a catenary support element. This element doesn’t follow the railway exactly along side, it crosses the rail line from side to side fig. 2.2b.

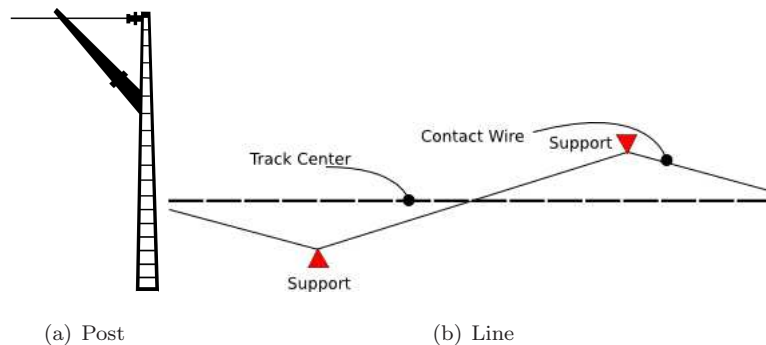


Figure 2.2: Catenary

2.3 The pantograph

The only objective of the pantograph is to collect electrical current from the catenary cable system.

2.3.1 Standard speed trains

Standard speed trains of about 100 Km/h, normally use old Catenary network systems. This type of train uses a pressure cushion, which makes the pantograph raise when it gains pressure or descend when it loses pressure.

At maximum speed these pantographs suffer from low contact force between registration strip and catenary, a deceiving higher calibration contact force doesn't solve the problem due to high wear in the contact system. A solution to this problem was successfully used by adding an aerodynamic wing to the pantograph registration strip, permitting the usage of lower calibration pressures giving better contact at higher speeds. The pantograph may or may not have passive elements depending on the supplier; passive elements aren't very common in standard low cost trains. Passive elements consist of spring and damper elements attached between bodies.



(a) Pantograph



(b) Train

Figure 2.3: Pantograph and train

2.3 The pantograph

2.3.2 High speed trains

According to *UIC* (*Union Internationale des Chemins de Fer*), "high-speed train" is a train that runs at over 250 km/h (*TGV* train) on dedicated tracks, or over 200 km/h (Pendular train) on upgraded conventional tracks. These trains are equipped with passive control regulators; depending on the velocity of the train the air cushion pressure gets regulated. These type of trains achieve high speeds because of the dedicated rail lines or of upgraded ones which involves great investment.

High speed trains still use the same technology as standard trains. In terms of pantograph it has to be manually calibrated and uses an air cushion. Passive elements are included to absorb high frequencies in the registration strip. An exception is the *Faiveley CX* version pantograph [15] fig. 2.4, these pantographs include force control for the contact force between the registration strip and wire to maintain the contact force in an admissible nominal value.



Figure 2.4: *Faiveley* pantograph *CX*

2.3.3 Force control pantograph on high speed train

Adding force control to conventional rail vehicles and making some upgrades to the rail lines (low cost upgrades to old rail lines) makes it possible to expand the usage of old rail lines with new or upgraded

trains. Normal trains could circulate faster in old railways; high speed trains in new rail lines could go even faster than the *TGV*'s 500 Km/h record in dedicated rails.

2.4 Passive pantograph limitations

Normal pantograph's are calibrated manually (figure 2.5) by a technician who sets the contact force by the standards of the catenary system regulations. Closed loop systems don't need manual calibration. Using high contact forces causes excessive wear in the pantograph, making possible for the registration strip to get stuck in the catenary cable. Low contact force can cause poor current collection resulting in electrical arcs which causes large damage to the catenary cable and pantograph registration strip.



Figure 2.5: Pantograph calibration

Chapter 3

Dynamics modelling in SimMechanics[®]

3.1 SimMechanics[®]

SimMechanics[®] is a tool for modelling and simulating mechanical systems, it's an extension to *Matlab*'s *Simulink* environment, using the newest and more robust mechanical modelling theory's adding it to *Simulink*'s efficient numerical solver. A comparison with other types of simulation applications can be seen in [7]. Although *SimMechanics* uses the most recent methods it still has it's bases on the Newton Euler Method. This application can handle relative or absolute coordinates to define the position of all element masses or joints. The orientation of these elements can be introduced using Euler rotation matrices or even quaternion. An overview on Matlab's potential and comparison to other alternatives is studied in [13].

The motion of bodies is described by its kinematics behavior. The dynamic behavior results due to the equilibrium of applied forces and the rate of change in the momentum. As an important feature, multibody system formalisms usually offer an algorithmic, computer-aided way to model,

3.2 Modelling multibody systems

analyze, simulate and optimize the arbitrary motion of possibly thousands of interconnected bodies. The advantage of using *SimMechanics*[®] is obvious, no formal mechanical formulations are directly required and the differential equations are automatically solved. The equations governing the motion of mechanical systems are typically higher-index differential algebraic equations (DAEs). *Simulink*[®] is currently designed to model systems governed by ordinary differential equations (ODEs) and a restricted class of index-1 DAEs. This chapter is based on a paper presented by *Mathworks*[®] for *SimMechanics*[®] [12, 16].

3.2 Modelling multibody systems

A multibody system is an abstract collection of bodies whose relative motions are constrained by means of joints. The representation of a multibody system is given by an abstract graph. The bodies are placed in direct correspondence with the nodes of the graph, and the constraints (where pairs of bodies interact) are represented by means of edges. Two fundamental types of systems exists, multibody systems whose graphs are acyclic, often referred to as tree topology systems, and multibody systems that give rise to cyclic graphs with closed-loops.

3.3 Relative versus absolute coordinate formulations

The structure of the equations of motion depends largely on the choice of coordinates. Many commercial software packages for multibody dynamics use the formulation in absolute coordinates. In this approach, each body is first assigned 6 degrees of freedom. Then, depending on the interaction of bodies due to joints, suitable constraint equations are formed. This results in a large number of configuration variables and relatively simple constraint equations, but also in a sparse mass matrix M .

This sparseness and the uniformity in which the equations of motions are derived is exploited by the software. However, due to the large number of constraint equations, this strategy is not suitable for *SimMechanics*®. It uses relative coordinates. In this approach, a body is initially given zero degrees of freedom. They are “added” by connecting joints to the body. Therefore, far fewer configuration variables and constraint equations are required. Acyclic systems can even be simulated without forming any constraint equations. The drawback of this approach is the dense mass matrix M , which now contains the constraints implicitly, and the more complex constraint equations.

3.4 Unconstrained systems

In this section we restrict attention to the class of multibody systems represented by noncyclic graphs, otherwise known as branched trees, by virtue of the fact that the graphs have the form of a rooted tree. For simplification purposes we further restrict attention to the subset of simple-chain systems. The results are easily extended to the more general case of branched trees but the analysis is much clearer in the case of simple chains. Simple chains are multibody systems where each body is connected to a unique predecessor body and a unique successor body (with the exception of the first and last bodies in the chain) by means of a joint. A common example is a robotic manipulator. In recent years, a number of techniques have appeared for solving the dynamics of these systems, ranging in computational complexity from $O(n)$ (where n is the number of bodies in the system) to $O(n^3)$

3.5 Analysis of simple chain systems

Consider the n -link serial chain in fig. 3.1, the tip of the chain to the base, which also acts as the inertial reference frame. Each body is connected to two joints, an inboard joint (closer to the base),

3.5 Analysis of simple chain systems

and an outboard joint (closer to the tip).

An arbitrary joint, the k^{th} joint, has an inboard side labelled O_k^+ attached to body $k+1$ and an outboard side labelled O_k attached to body k . The center of mass on the k^{th} body is denoted by $p(k)$, and the vector from O_k to O_{k-1} is denoted by $r(k, k-1)$. This vector plays an important role in shifting forces and velocities between bodies.

The spatial velocity $V(k) \in \mathbb{R}^6$ at the outboard side of the k^{th} joint is defined by

$$V(k) = [w(k)^T, v(k)^T]^T,$$

where $w(k) \in \mathbb{R}^3$ is the angular velocity of the k^{th} body and $v(k) \in \mathbb{R}^{3 \times 3}$ is the linear velocity of the k^{th} body at the point O_k . Here we assume that both vectors are expressed in inertial coordinates.

The spatial force $f(k) \in \mathbb{R}^6$ applied by the k^{th} joint to the k^{th} body at the point $O(k)$ is defined by $f(k) = [T(k)^T, F(k)^T]^T$, where $T(k) \in \mathbb{R}^3$ is the applied torque and $F(k) \in \mathbb{R}^3$ is the applied force, again expressed in inertial coordinates.

The spatial inertia matrix $M(k)$ is defined as

$$M(k) = \begin{bmatrix} J(k) & m(k)\tilde{p}(k) \\ -m(k)\tilde{p}(k) & m(k)I_3 \end{bmatrix} \in \mathbb{R}^{6 \times 6}; \quad (3.1)$$

where $m(k)$ is the mass of the k^{th} body, and $J(k) \in \mathbb{R}^3$ is the inertia tensor of the k^{th} body about the center of mass, computed in inertial coordinates. Given a vector $p \in \mathbb{R}^{3 \times 3}$ we let $\tilde{p} \in \mathbb{R}^3$ denote the cross product matrix generated from the vector p . Thus $\tilde{p}(k)$ denotes the cross product matrix generated from $p(k)$. Denote the time derivative of $V(k)$ by $\alpha(k)$. The following kinematics equations describe the motion of the chain:

$$V(k) = \phi^T(k+1; k)V(k+1) + H^T(k)\dot{q}(k), V(n+1) = 0, k = n, n-1, \dots, 1 \quad (3.2)$$

$$\alpha(k) = \phi^T(k+1; k)\alpha(k+1) + H^T(k)\ddot{q}(k) + a(k), \alpha(n+1) = 0, k = n, n-1, \dots, 1 \quad (3.3)$$

Here, $q(k) \in \mathbb{R}^{n_{nq}}$ is the vector of configuration variables for the k th joint, the columns of $H^T(k) \in \mathbb{R}^{6 \times n_{nq}}$ span the relative velocity space between the k^{th} body and the $(k+1)^{th}$ body, and $\phi^T(k+1; k)$ is the transpose of the matrix

$$\phi(k+1, k) = \begin{bmatrix} I_3 & \dot{r}(k+1, k) \\ 0 & I_3 \end{bmatrix} \quad (3.4)$$

where the vector $r(k+1, k)$ is the vector from the outboard side of the $(k+1)^{th}$ joint to the outboard side of the k th joint. The vector $a(k) \in \mathbb{R}^6$ represents the Coriolis acceleration of the k th body and is given by

$$a(k) = \begin{bmatrix} \tilde{w}(k+1)w(k) \\ \tilde{w}(k+1)(v(k) - v(k+1)) \end{bmatrix} \quad (3.5)$$

Given the joint velocity degrees of freedom (DoFs) $\dot{q}(k)$ and acceleration DOF $\ddot{q}(k)$, these equations provide a simple recursive procedure for determining the velocities and accelerations of the bodies constituting the chain. The equations of motion, formulated about the reference points $O(k)$, are

$$\begin{aligned} f(k) &= \phi(k, k-1)f(k-1) + M(k)\alpha(k) + b(k) \\ f(k) &= \phi(k, k-1)f(k-1) + M(k)\alpha(k) + b(k)T(k) = H(k)f(k) \end{aligned} \quad (3.6)$$

We can express these recursive relationships in matrix form as follows. Using the sum of the velocity recursion and the fact that $\phi(i, i) = I_6$ and $\phi(i, k)\phi(k, j) = \phi(i, j)$. The second relationship follows from the fact that shifting a spatial force from O_j to O_k and then from O_k to O_i is equivalent to shifting the force directly from O_j to O_i . Then

$$V(k) = \sum_{i=1}^n \phi^T(i, k)H^T(i)\dot{q}_i \quad (3.7)$$

A natural definition of the matrix operators follows:

$$H^T = \text{diag}[H^T(1), \dots, H^T(n)] \quad (3.8)$$

3.5 Analysis of simple chain systems

The operator ϕ is defined by:

$$\phi = \begin{bmatrix} I_{6 \times 6} & 0 & \dots & 0 \\ \phi(2, 1) & I_{6 \times 6} & \dots & 0 \\ \vdots & \vdots & \ddots & \vdots \\ \phi(n, 1) & \phi(n, 2) & \dots & I_{6 \times 6} \end{bmatrix} \quad (3.9)$$

In terms of the matrix ϕ , the velocity and force recursions can be written as

$$V = \phi^T H^T \dot{q} \quad (3.10)$$

$$\alpha = \phi[H^T \ddot{q} + a] \quad (3.11)$$

$$f = \phi[M\alpha + b] \quad (3.12)$$

$$T = Hf \quad (3.13)$$

where the spatial velocity vector V is defined as $V^T = [V^T(1), V^T(2), \dots, V^T(n)] \in \mathbb{R}^{6n}$, and similarly for the spatial acceleration vector $\alpha \in \mathbb{R}^{6n}$, the Coriolis acceleration vector $a \in \mathbb{R}^{6n}$, the gyroscopic force vector $b \in \mathbb{R}^{6n}$, and the spatial force vector $f \in \mathbb{R}^{6n}$. Finally the matrix $M \in \mathbb{R}^{6 \times 6}$ is defined to be $M = \text{diag}[M(1), M(2), \dots, M(n)]$. Substituting into the last equation, we obtain the equations of motion:

$$T = H\phi M \phi^T H^T \ddot{q} + H\phi[M\phi^T a + b] \quad (3.14)$$

This equation is in a factorized form, and its structure may be exploited to obtain a global or recursive solution.

In the simulation problem, the motion of a mechanical system is calculated based on the knowledge of the torques and forces applied by the actuators, and the initial state of the machine:

1. The forward dynamics problem in which the joint accelerations are computed given the actuator torques and forces.

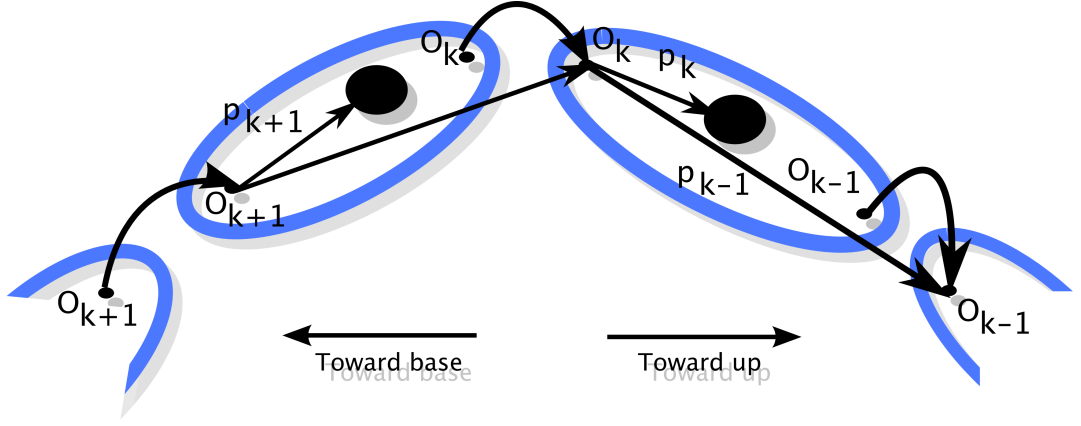


Figure 3.1: Bodies and joints in a serial chain

2. The motion integration problem in which the joint trajectories are computed based on the given acceleration.

Several computational techniques have been developed for the forward dynamics problem. Most of them are recursive methods. Two popular ones are the $O(n^3)$ Composite Rigid Body Method (CRBM) and the $O(n)$ Articulated Rigid Body Method (ABM) which are derived in [17]. The ABM uses the sparsity structure of large systems with many bodies (> 7) efficiently, but produces more computational overhead than the CRBM which can be preferable for smaller systems. The computational cost of the forward dynamics problem is only half the story, however. The characteristics of the resulting equations also have an influence on the performance of the adaptive time-step ODE solvers of Simulink (“formulation stiffness”). The ABM often produces better results, especially for ill-conditioned problems [18].

For unconstrained systems, the application of the CRBM and ABM methods, and the following integration of the ODEs is straightforward. A simulation program, however, must be able to handle arbitrary mechanisms. In *SimMechanics*®, cyclic systems are reduced to open topology systems by

3.6 Linearization

cutting joints, which are (mathematically) replaced by a set of constraint equations. They ensure, that the system with the cut joints moves exactly as the original cyclic mechanism. The user can choose if he wants to select the cut-set by himself or if he leaves this task to *SimMechanics*[®]. Of course, the structure of the resulting equations depends largely on this choice. In all cases, however, the equations of motion of constrained systems are index-3 DAEs, which have to be transformed into ODEs in order to be solvable with the *Simulink*[®] ODE solver suite.

The approach taken by *SimMechanics*[®] is to differentiate the constraint equation twice and solve for the Lagrange multiplier, λ . Near singularities of the mechanism, i.e. near points where the number of independent constraint equations is decreased and the solution for λ is no longer unique, numerical difficulties arise. To deal with this problem, the user chooses between two solvers. One, based on Cholesky decomposition (the default), which is generally faster, and one based on QR decomposition, which is more robust in the presence of singularities [19].

3.6 Linearization

A linearized model is an approximation to a nonlinear system, which is valid in a small region around the operating point of the system. Engineers often use linearization in the design and analysis of control systems and physical models. The following figure shows a visual representation of a nonlinear system as a block diagram. The diagram consists of an external input signal, $u(t)$, a measured output signal, $y(t)$, and the nonlinear system that describes the system's states and its dynamic behavior, P .

It is possible to express a nonlinear system in terms of the state space equations

$$\dot{x}(t) = f(x(t), u(t), t) \quad (3.15)$$

$$y(t) = g(x(t), u(t), t) \quad (3.16)$$

where $x(t)$ represents the system's states, $u(t)$ represents the inputs, and $y(t)$ represents the outputs.

In these equations, the variables vary continuously with time.

A linear time-invariant approximation to this nonlinear system is valid in a region around the operating point at $t = t_0, x(t_0) = x_0, u(t_0) = u_0$ if the values of the system's states, $x(t)$ and inputs, $u(t)$ are close enough to the operating point. To describe the linearized model, it helps to first define a new set of variables centered about the operating point of the states δx , inputs δu , and outputs δy .

Simulink uses a series of connected blocks to model physical systems and control systems. Input and output signals connect the blocks, which represent mathematical operations. The nonlinear system, P, in fig. 3.2, hides a series of connected Simulink blocks.

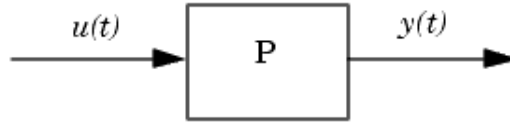


Figure 3.2: Plant to linearize

Simulink linearizes both continuous and discrete-time nonlinear systems by computing the state-space matrices of the linearized model, A, B, C, and D, using a *Block-by-Block Analytical Linearization* or a *Numerical – Perturbation Linearization*.

The linearized state space equations written in terms of $\delta x(t)$, $\delta u(t)$ and $\delta y(t)$ are

$$\dot{x}(t) = A\delta x(t) + B\delta u(t) \quad (3.17)$$

$$y(t) = C\delta x(t) + D\delta u(t) \quad (3.18)$$

where A, B, C, and D are constant coefficient matrices. These matrices are defined as the Jacobians

3.6 Linearization

of the system, evaluated at the operating point

$$A = \frac{\partial f}{\partial x}|_{t_0, x_0, u_0} \quad B = \frac{\partial f}{\partial u}|_{t_0, x_0, u_0} \quad (3.19)$$

$$(3.20)$$

$$C = \frac{\partial g}{\partial x}|_{t_0, x_0, u_0} \quad D = \frac{\partial g}{\partial u}|_{t_0, x_0, u_0} \quad (3.21)$$

The transfer function representation may also be obtained. To this end we apply the Laplace transform to eq. 3.18 and eq. 3.18 and manipulate to obtain, provided $(x_0, u_0) = (0, 0)$

$$\frac{Y(s)}{U(s)} = P_{lin}(s) = C(sI - A)^{-1}B + D$$

Where s is the Laplace variable and I is the identity matrix.

Chapter 4

SimMechanics[®] pantograph model

A pantograph (see fig. 4.1) consists of a collection of bodies and mechanical elements attached to a railway carbody that is moving along the track. Due to their structural stiffness, the components that compose the pantograph are considered here as rigid bodies. These bodies are connected by a set of kinematic joints, responsible to control their relative motion, and by a group of rigid and/or flexible elements. These elements are used to model the relevant internal forces resulting from the interaction among bodies of the system.

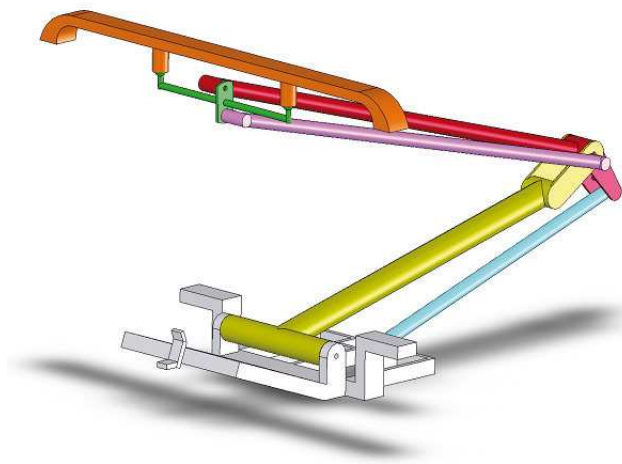


Figure 4.1: The pantograph

4.1 Pantograph body elements

4.1.1 Basic components

The pantograph model is such that the origin of the pantograph reference frame (x, y, z) is the insertion point on the carbody. A local reference frame (ξ, η, ζ) is rigidly attached to the center of mass (CM) of each body of the pantograph and its spatial orientation is such that the axes are aligned with the principal inertia directions of the rigid bodies. Therefore, the inertia tensor of each body is completely defined by the inertia moments $(I_\xi \ I_\eta \ I_\zeta)$.

The pantograph is composed by seven rigid elements (figure 4.2):

- | | | | |
|---|------------|---|---------------------------|
| 1 | Base | 5 | Top link |
| 2 | Lower arm | 6 | Stabilization armTop link |
| 3 | Top arm | 7 | Registration strip |
| 4 | Lower link | | |

The initial position and initial orientation of each body in the system is given, respectively, by the location of it's *CM* and by the orientation of it's local reference frame (ξ, η, ζ) with respect to the pantograph reference frame (x, y, z) . The inertia properties with respect to the three principal axes (I_ξ, I_η, I_ζ) are presented in table 4.1, the initial position and the initial orientation of each rigid body are presented in table 4.2 were e_0 are the Euler angles. The data presented in this section is from the CX pantograph.

4.1.2 Passive elements

Passive elements are spring and dampers which are placed in the registration strip to absorb the catenary dynamics (figure 4.3). Furthermore, there is a spring damper element at the base joint.

These elements are also considered force elements that are transmitted among the rigid bodies that

ID	Name	Mass (Kg)	Inertia ($Kg.m^2$)		
			$[I_\xi \quad I_\eta \quad I_\zeta]$		
1	Base	32.65	2.7600	4.8700	2.3110
2	LowerArm	32.18	0.3060	10.4300	10.6500
3	TopArm	15.6	0.1470	7.7630	7.8620
4	LowerLink	3.10	0.0500	0.4560	0.4560
5	TopLink	1.15	0.0500	0.4790	0.4790
6	StabilizationArm	1.51	0.0700	0.0500	0.0690
7	RegistritionStrip	9.50	1.5920	0.2080	1.7770

Table 4.1: Rigid body mass and inertia

ID	Name	$P_0(m)$	$e_0(m)$
1	Base	5 0 3	0 0 0
2	LowerArm	4.4295 0 3.4125	0 0.1737 0
3	TopArm	4.6059 0 4.0555	0 -0.1818 0
4	LowerLink	4.1135 0 3.2833	0 0.2105 0
5	TopLink	4.6428 0 4.0025	0 -0.1639 0
6	StabilizationArm	5.5529 0 4.4180	0 0 0
7	RegistritionStrip	5.5529 0 4.5080	0 0 0

Table 4.2: Rigid body initial position and orientation

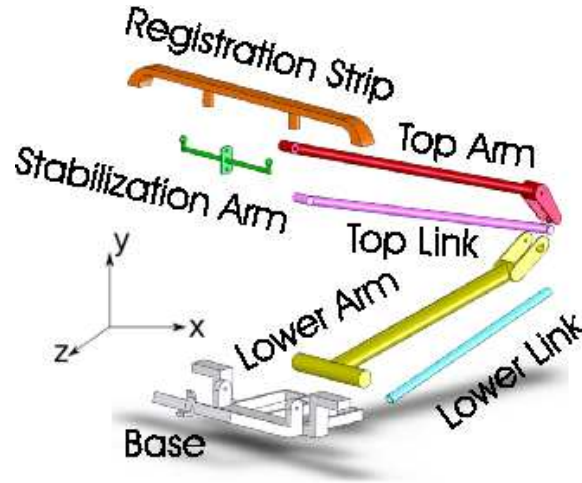


Figure 4.2: Pantograph elements

compose the pantograph system. The stiffness K , natural length l and damping C characteristics of these elements, the numbers of bodies that they connect and the local coordinates of the attachment points are presented in table 4.3.

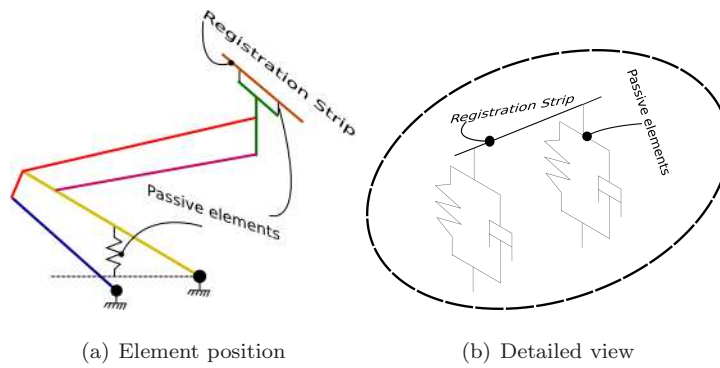


Figure 4.3: Passive elements

4.1.3 Active elements

The pantograph active element is a pneumatic cushion which raises or lowers the contact interface (registration strip) depending on its internal pressure. Calibration of this element is made by a technician who sets the contact force to a standard catenary operation value. This is an actuating element thus a control input variable.

ID i linked to ID j	Body [i j]	P_i [x y z] (m)	P_j [x y z] (m)	[K l C] (N/m, m, Ns/m)
ID 1 - ID 2	[1 2]	[-0.5705 0 0]	[0 0 0]	[1000 0.4131 3000]
ID 6 - ID 7	[6 7]	[0 0.3350 0]	[0 0.3350 0]	[3600 0.1033 13]
ID 6 - ID 7	[6 7]	[0 -0.3350 0]	[0 -0.3350 0]	[3600 0.1033 13]

Table 4.3: Passive elements information

4.1.4 Joints

These elements make the connection between body elements. There are three basic types of joints: prismatic (1 linear *DOF*), revolute (1 angular *DOF*) or spherical (3 angular *DOF*), their position can be seen in figure 4.4; with these basic joints more complex joints can be obtained by combining them (figure 4.5). Standard pantographs have only revolute joints, new pantographs have revolute and spherical joints. Spherical joints add extra *DOF*, which means that when the registration strip gets stuck, in the catenary cable, the pantograph isn't ripped out of the train roof.

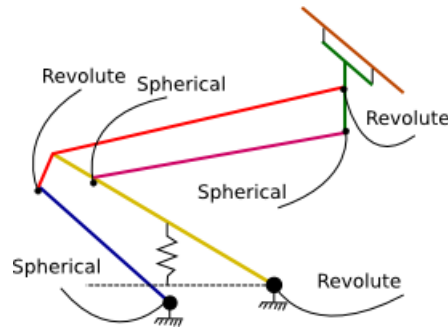


Figure 4.4: Joint positioning

4.2 Physical modelling blocks

SimMechanics® blocks do not directly model mathematical functions but have a definite physical meaning. The block set consists of block libraries for bodies, joints, sensors and actuators, constraints and drivers, and force elements. Besides simple standard blocks there are some blocks with advanced

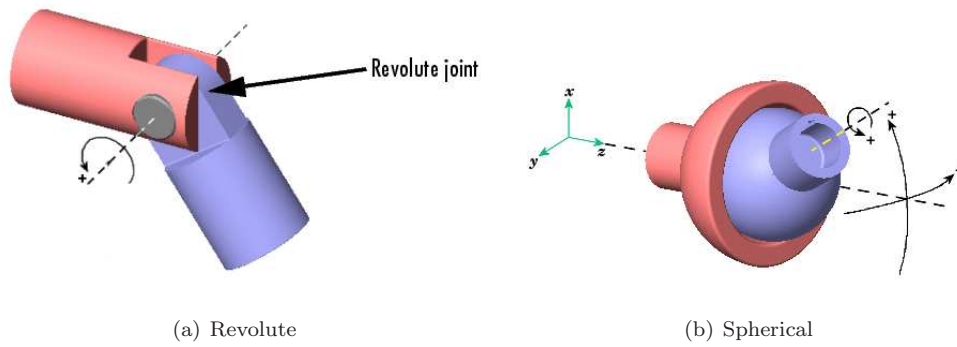


Figure 4.5: Joints (SimMechanics® representation)

functionality available, which facilitate the modelling of complex systems enormously. Another feature are Disassembled Joints for closed loop systems. If a machine with a closed topology is modelled with such joints, the user does not need to calculate valid initial states of the system by solving systems of nonlinear equations. The machine is assembled automatically at the beginning of the simulation.

4.3 Major Steps of the Dynamical Analysis

This section summarizes the steps carried out by *SimMechanics*® during machine simulation. It is based on chapter 5 of [16].

1.
 - Check of data entries in dialog boxes.
 - Validation of body, joint, constraint, driver geometry, and model topology.
2.
 - Check of assembly tolerances.
 - Cutting of closed loops, formulation of constraint equations, and check for consistency and redundancy of constraints.
 - Examination of Joint Initial Condition blocks, assembly of disassembled joints, and again check of assembly tolerances.

- Mode iteration for sticky joints.
3. • Forward Dynamics/ Trimming modes: Application of external torques and forces. Formulation and integration of the equations of motion and solution for machine motion.
- Inverse Dynamics/ Kinematics modes: Application of motion constraints, drivers, actuators. Formulation of equations of motion and solution for machine motion and actuator torques and forces.
 - After each time step in all analysis modes: check of assembly, constraint, and solver tolerances, constraint and driver consistency and joint axis singularities.

4.4 Creating a Pantograph in SimMechanics[®]

4.4.1 Initial configurations

To create a nonlinear model in SimMechanics[®], it is necessary to have Matlab[®] and Simulink[®] installed. In the Simulink[®] “Parameters” menu a numeric solver is already configured by default.

The numeric solver that was used is a variable step Dormand-Prince algorithm (see fig. 4.6)).

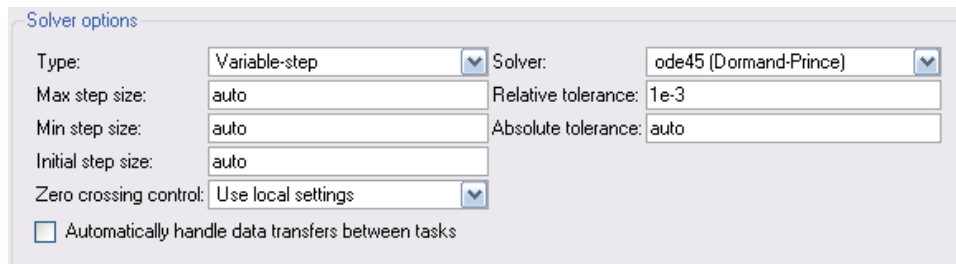


Figure 4.6: SimMechanics: Parameters

The main work in this project was done in continuous time, but some test were made with discrete controllers although not presented in this work, thus instead of variable step a fixed step solver was used with a sample time of 0.001 seconds with a discrete solver. The sample time for the discrete

4.4 Creating a Pantograph in SimMechanics®

solver was obtained by finding the linear model poles of the open loop system. The most distant pole found in successive model analysis was of 35 rad/s (see eq. 4.4.1).

$$T = \frac{1}{f}, \quad f = \frac{w}{2\pi}, \quad \text{sample time} = \frac{1}{20f}$$

For convenience, instead of the value obtained which is 0.00879 s , a more regular value for the sample time is used, the value is 1 ms .

$$\text{sample time} = .00879 \approx 0.001 \text{ s}$$

4.4.2 Linking the data file to the SimMechanics® model

Before it is possible to deliver the necessary information to every element in the SimMechanics model, it is necessary to add a translation interface between the information and the blocks. Organizing the data in a Matlab structure variable (figure 4.7) is very useful; it's possible to reference every important information in a single variable which then is linked to the SimMechanics model. The data file is linked to the model and the variable is generated automatically when the Simulink model starts. Modifying any element in the data file will alter the correspondent mechanical element in the model.

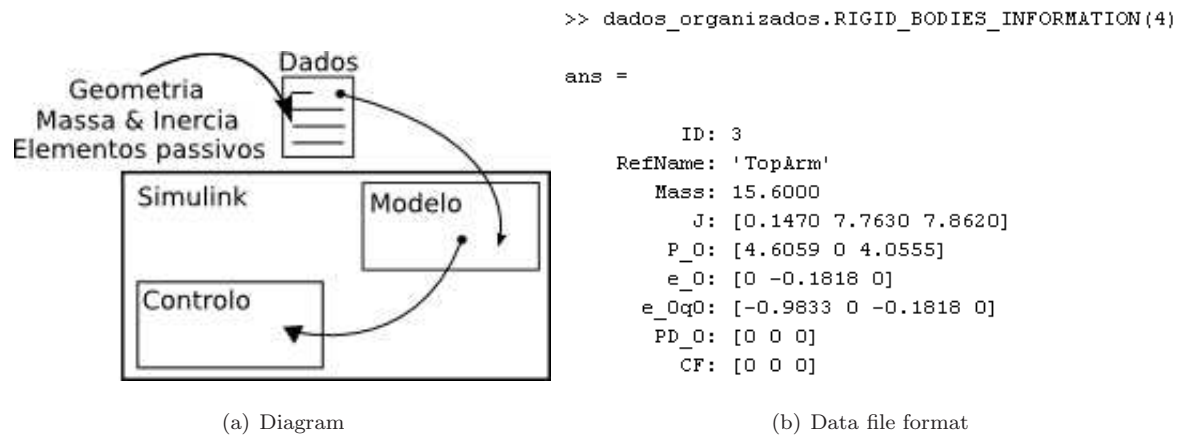


Figure 4.7: Data model

4.4.3 SimMechanics® pantograph model

SimMechanics® is specially equipped for easy model creation, all the necessary block elements for model creation are presented in the SimMechanics® Block Toolset. The primary rule for model creation is that a body block has to be followed by a joint block. Reference frames are very important for model creation, and choosing between global coordinates or local coordinates is allowed. In figure 4.8 the data structure in a body element is presented, position and orientation have to be introduced. Mass and inertia values are also introduced in this element box (4.9).

Position		Orientation				
Show Port	Port Side	Name	Orientation Vector	Units	Relative CS	Specified Using Convention
<input checked="" type="checkbox"/>	Top	CG	dados_organizados.	deg	World	Quaternion
<input checked="" type="checkbox"/>	Bottom	CS4	[0 0 0]	deg	World	Euler X-Y-Z
<input checked="" type="checkbox"/>	Bottom	CS6	[0 0 0]	deg	World	Euler X-Y-Z
<input checked="" type="checkbox"/>	Bottom	CS1	[0 0 0]	deg	World	Euler X-Y-Z
<input type="checkbox"/>	Top	CS5	[0 0 0]	deg	World	Euler X-Y-Z
<input checked="" type="checkbox"/>	Top	CS3	[0 0 0]	deg	World	Euler X-Y-Z
<input checked="" type="checkbox"/>	Top	CS2	[0 0 0]	deg	World	Euler X-Y-Z

Figure 4.8: Generic mass data

Block Parameters: Lower Arm

Body

Represents a user-defined rigid body. Body defined by mass m , inertia tensor I , and coordinate origins and axes for center of gravity (CG) and other user-specified Body coordinate systems. This dialog sets Body initial position and orientation, unless Body and/or connected Joints are actuated separately.

Mass properties

Mass: dados_organizados.RIGID_BODIES_INFORMATION(3)Mass kg

Inertia: diag(dados_organizados.RIGID_BODIES_INFORMATION(3)J) kgm^2

Position

Orientation

Show Port	Port Side	Name	Origin Position Vector [x y z]	Units	Translated from Origin of	Components in Axes of
<input checked="" type="checkbox"/>	Top	CG	dados_organizados.	m	World	World
<input checked="" type="checkbox"/>	Bottom	CS4	[0 0 0]	m	CG	CG
<input checked="" type="checkbox"/>	Bottom	CS6	[0 0 0]	m	CG	CG
<input checked="" type="checkbox"/>	Bottom	CS1	[0 0 0]	m	Adjoining	Adjoining
<input type="checkbox"/>	Top	CS5	dados_organizados.	m	CG	CG
<input checked="" type="checkbox"/>	Top	CS3	dados_organizados.	m	CG	CG
<input checked="" type="checkbox"/>	Top	CS2	dados_organizados.	m	CG	CG

OK Cancel Help Apply

Figure 4.9: Mass orientation

4.4.4 The catenary model

There are several approaches for catenary modelling. Obtaining the dynamical model is a very hard task because the behavior of the catenary depends upon the direct influence of the pantograph, weather conditions, train suspension and other unknown factors. Furthermore, the catenary is composed by a cable system which is considered a flexible element and has it's own modes of vibration. One type of approach is based on finite element modelling. In this approach cable flexibility is considered, but it is a very complex method to formulate the dynamical system equations. Because the objective is to control the pantograph, it is possible to be less precise in the catenary model, formulating the catenary element as it were a perturbation to the pantograph. This approach simplifies greatly the task of creating the whole system model. The catenary is used also as a force sensor measuring the force value, allowing to have a simple yet easy output contact force measure.

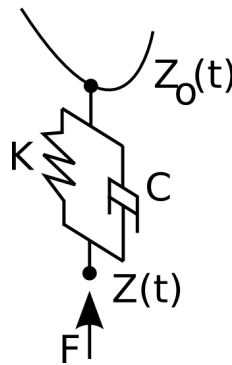


Figure 4.10: Equivalent model of the Catenary

The catenary model is a spring - damper system. These two elements are used in the z direction and in the y direction, both are placed in the center of the registration strip. This is a simplification of the system meaning that the pantograph only has one degree of freedom. The implementation is simple, it uses a parallel association of a spring and a damper elements. To simulate Catenary perturbation (force variations) passive element displacement is used that generate as a result force

variations. The implementation follows in figure 4.11 and it's global positioning in the pantograph.

$$F = K [z - z_0(t)] + C [\dot{z} - \dot{z}_0(t)] \quad (4.1)$$

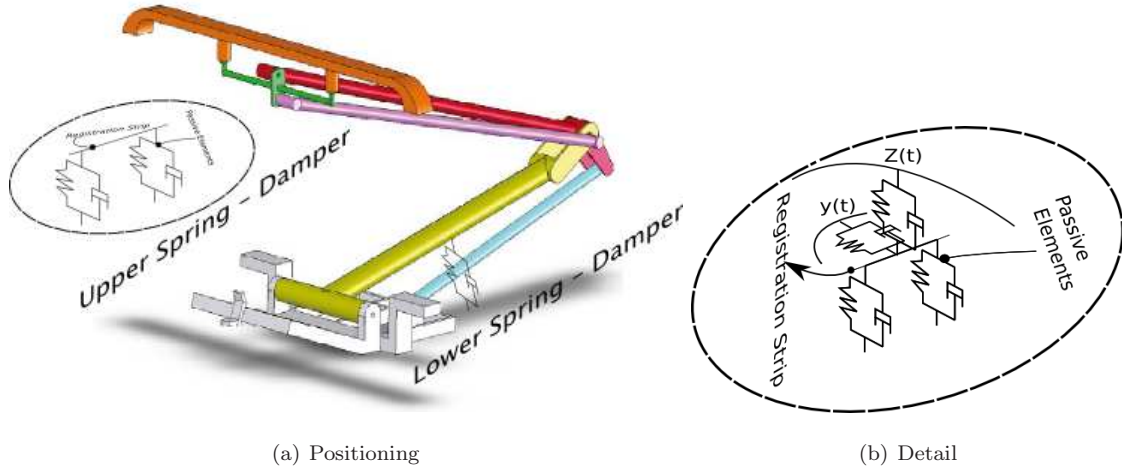


Figure 4.11: Catenary representation

An important note is that K and C (spring and damper constants) can be altered in time which can make the simulation more realistic. To simplify the model, K and C were considered constant over time. Furthermore, F is the contact force between the pantograph and the catenary. The position z is the height of the registration strip and z_0 is the initial position of the registration strip.

4.5 Pantograph models

A correct model of the pantograph means that the contact interface has to be as realistic as possible. A progressive complexity approach was used to obtain the nonlinear model and thus the pantograph dynamics. Nonlinear models are more complex to study, and in order to simplify the system, linearization is used. All linear models are obtained in the nominal conditions, the process can be seen in figure 4.12.

In order to analyze the pantograph five different types of pantographs are studied. Model and

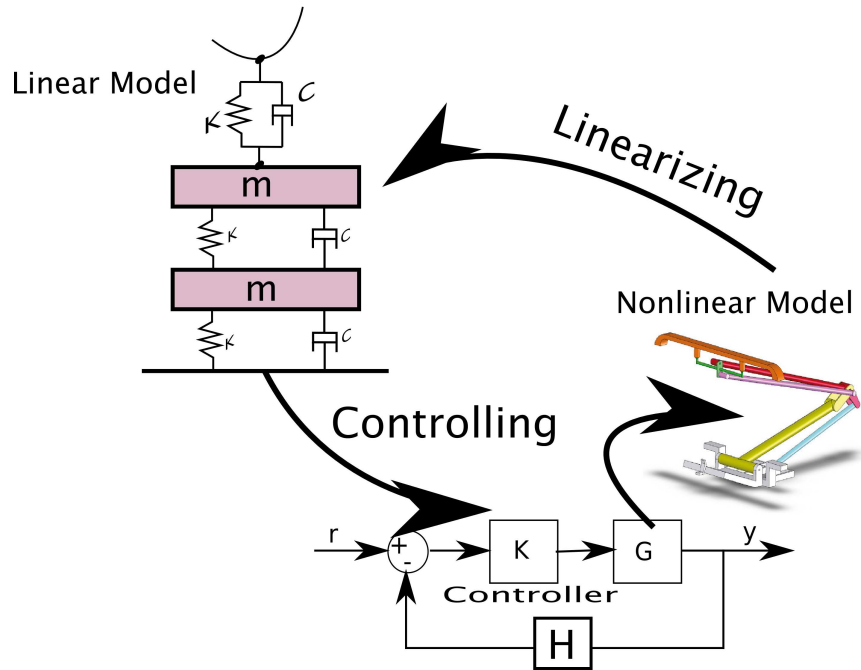


Figure 4.12: Linearization process for control

controllers are developed and performance and robustness analyzed. In figure 4.13 the model types are presented and in table 4.4 it is possible to see model properties, F_c represents the catenary force, M is the torque applied by the actuator, and F_a is the registration strip actuator force.

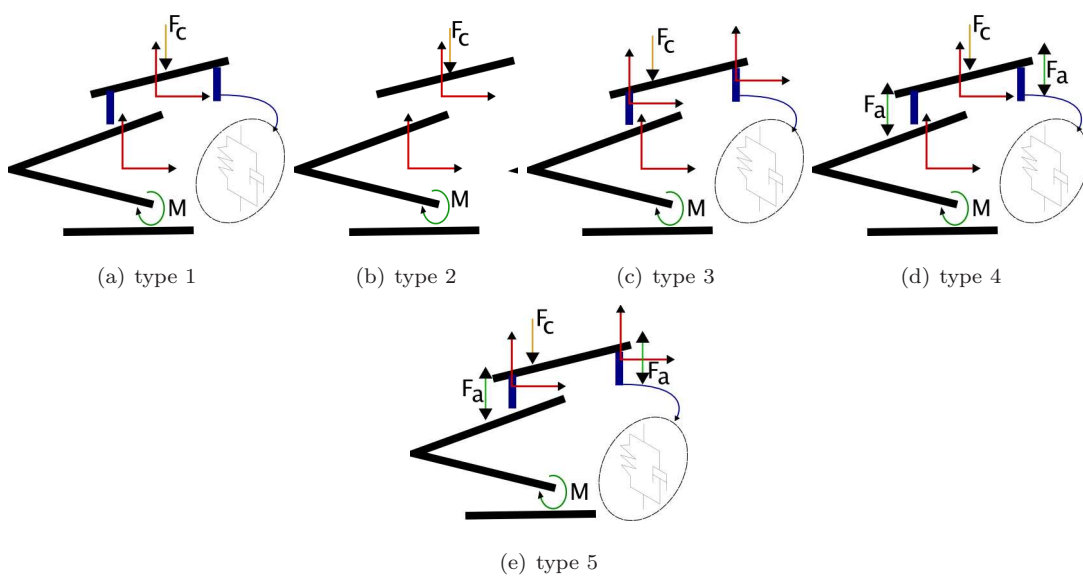


Figure 4.13: Pantograph configurations studied

	Motion	DOF	Actuator	Upper passive elements
Type 1	Plane	2	1	present
Type 2	Plane	1	1	not present
Type 3	Spacial	3	1	present
Type 4	Plane	2	2	present
Type 5	Spacial	3	3	present

Table 4.4: Pantograph model type considerations

4.6 Linearization and Trimming in SimMechanics[®]

The linearization and trimming functionalities for SimMechanics models are equivalent to traditional Simulink systems. The *linmod* command derives an LTI state space model in the form

$$\dot{x}(t) = Ax(t) + Bu(t) \quad (4.2)$$

$$y(t) = Cx(t) + Du(t) \quad (4.3)$$

where x is the model's state vector, y is its outputs, and u is its inputs as previously. The trim command finds solutions for the model that satisfy specified conditions on its inputs, outputs, and states, e.g. equilibrium positions where the system does not move, or steady state solutions where the derivatives of the systems states are zero. In order to use both commands, the initial states of the system have to be specified. All models designed for forward dynamics can be linearized. For trimming, on the contrary, one has to enter the Trimming mode. This causes SimMechanics[®] to insert a subsystem into the model in order to deal with the position and motion constraints. Because the catenary isn't modelled in *SimMechanics*[®] linearization for the whole system isn't possible. Linearization was done using alternative resources present in the *Matlab Control Toolbox*[®].

4.7 Visualization Tools

SimMechanics[®] offers two ways to visualize and animate machines. One is the build-in Handle Graphics tool, which uses the standard Handle Graphics facilities known from Matlab with some special features unique to *SimMechanics*. It can be used while building the model as a guide in the assembly process. If a body is added or changed in the block diagram, it is also automatically added or changed in the figure window. This gives immediate feedback and is especially helpful for new users or for complex systems. The visualization tool can also be used to animate the motion of the system during simulation. This can be much more expressive than ordinary plots of motion variables over time. The drawback is a considerably increased in computation time if the animation functionality is used. The bodies of the machine can be represented as convex hulls. These are surfaces of minimum area with convex curvature that pass through or surrounds all of the points fixed on a body. The visualization of an entire machine is the set of the convex hulls of all its bodies. More realistic renderings of bodies are possible if the *Virtual Reality Toolbox*[®] for *Matlab*[®] is installed. Arbitrary virtual worlds can be designed with the Virtual Reality Modelling Language (VRML) and interfaced to the *SimMechanics*[®] model.

4.8 Virtual model and world creation

The main application for model building and world creation is VR Builder. This is an old application but it's the application that is bundled with Matlab. The problem of creating the pantograph's elements in VR Builder is that it isn't a very good element creator. To bypass this problem the usage of SolidWorks for element creation makes it an easier solution for the creation of individual pantograph elements; this approach has the advantage of using some of SolidWorks[®] advanced functions for

kinematic study. The limitation of this approach is the position of the designated reference frame in both applications. Importing data can cause reference frame changes. If the user isn't cautious in the positioning, later usage of the element built in SolidWorks can be more complex. Importing all elements to VRML Builder is the first step to obtain the VRML model presented in fig. 4.14.

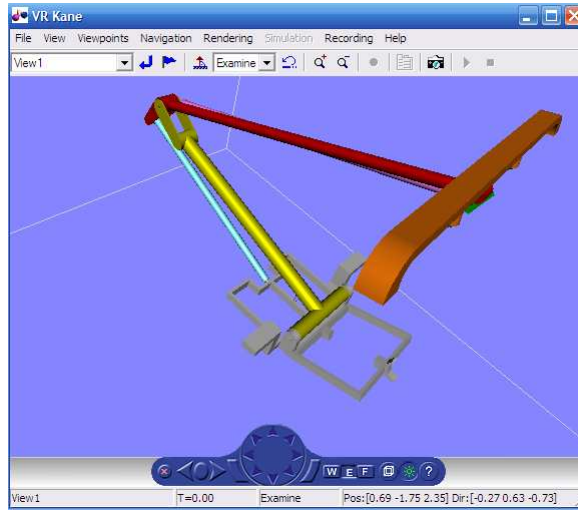


Figure 4.14: VRML model

4.9 SimMechanics® VRML model integration

VRML model linking is based on the connection of each joint to the corresponding SimMechanics model joint. A representation of how elements are linked to each other is presented in fig. 4.15.

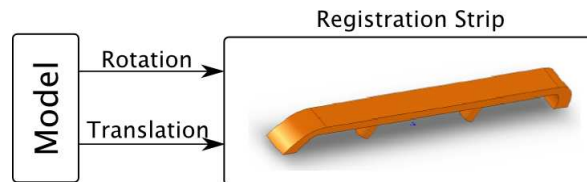


Figure 4.15: Linking SimMechanics with VR Sink

In these block we have the SimMechanics output sensor sources which will enter the VR Sink block. Because model references are different, rotation and position corrections have to be made (fig. 4.16) in order to make compatible VRML model and SimMechanics coordinate systems.

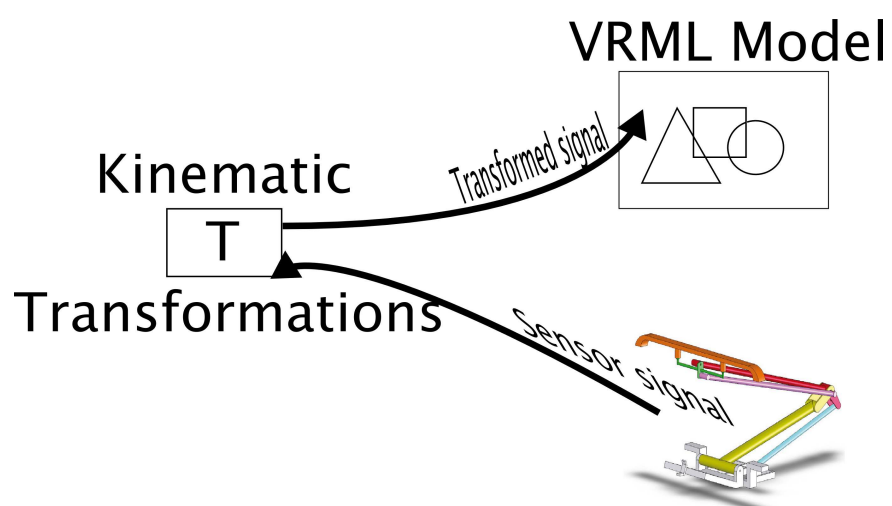


Figure 4.16: SimMechanics model connection to VRML model

Chapter 5

Pantograph control

One of the performance objectives of controller design is to keep the error between the controlled output and the set-point as small as possible, when the closed-loop system is affected by external signals. In this chapter, we will take a brief look at one such quantifying measure, the sensitivity function and its counterpart, the complementary sensitivity function. In the case of a conventional closed-loop system, the sensitivity function relates to disturbance rejection properties while the complementary sensitivity function provides a measure of set-point tracking performances. Furthermore, through the relationship between these two functions, we often have to sacrifice one aspect in favor of the other. From the sensitivity functions, we know that perfect control can never be achieved in practice. In fact compromises are often made between performance and stability, between excessive sensitivity to noise and achievement of control objectives, between good set-point tracking and good disturbance rejection. Because of all the compromises that may have to be made in assessing the performance of any particular scheme, we therefore have to answer the question as to how "good" the implemented control is.

This chapter, is also intended to explain the types of control strategies implemented in the panto-

5.1 Introduction to robust controllers

graph. A simple *PID* controller was implemented as a term of comparison with the robust controllers developed. Two types of robust controllers were studied H_2 and H_∞ . A key reason for using feedback is to reduce the effects of uncertainty which may appear in different forms as disturbances or as other imperfections in the models used to design the feedback law. Model uncertainty and robustness have been a central theme in the development of the field of automatic control. H_2 or H_∞ control techniques belong to a wider class of robust control techniques. The aim of this class of controllers is to prevent the negative consequences on closed-loop performances of uncertainties affecting the plant model.

5.1 Introduction to robust controllers

5.1.1 Robust control preliminaries

From [20], "Robust control refers to the control of unknown plants with unknown dynamics subject to unknown disturbances". Clearly, the key issue with robust control systems is uncertainty and how the control system can deal with this problem. Figure 5.1 shows an expanded view of the simple control loop. Uncertainty is shown entering the system in three places. There is uncertainty in the model of the plant. There are disturbances that occur in the plant system. Also there is noise which is read on the sensor inputs. Each of these uncertainties can have an additive or multiplicative component.

From fig. 5.1 we can see the separation of the computer control system with that of the plant. It is important to understand that the control system designer has little control of the uncertainty in the plant. The designer creates a control system that is based on a model of the plant. However, the implemented control system must interact with the actual plant, not the model of the plant.

Robust control methods seek to bound the uncertainty rather than express it in the form of a

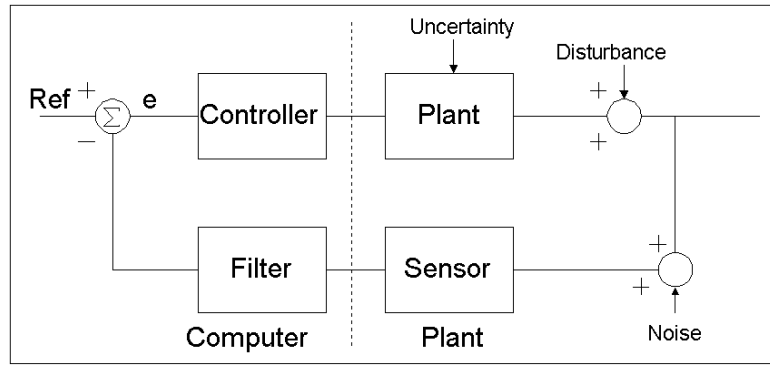


Figure 5.1: Simple control loop system with uncertainty

distribution. Given a bound on the uncertainty, the control can deliver results that meet the control system requirements in all cases. therefore, robust control theory might be stated as a worst-case analysis method rather than a typical case method. It must be recognized that some performance may be sacrificed in order to guarantee that the system meets certain requirements. However, this seems to be a common theme when dealing with safety critical embedded systems.

One of the most difficult parts of designing a good control system is modelling the behavior of the plant which in is the pantograph we are studying. There are a variety of reasons for why modelling is difficult.

- Imperfect plant data - Often, little data is available about the plant. Many control systems are designed concurrently with the plant. Even if there are similar plants in existence, each plant is slightly different because of the tolerances associated with individual components.
- Time varying plants - The dynamics of some plants vary over time. A fixed control model may not accurately depict the plant at all times.
- Higher order dynamics - Some plants have a high frequency dynamic that is often neglected in the nominal plant model. For instance, vibration may cause unwanted affects at high frequencies.

Sometimes this dynamic is unknown and sometimes it is deliberately ignored in order to simplify the model.

- Non-linearity - Most control systems are designed assuming linear time invariant systems. This is done because it greatly simplifies the analysis of the system. However, all of the systems encountered in the real world have some non-linear component. Thus the model will always be an approximation of the real world behavior.
- Complexity - Mechanical and electrical systems are inherently complex to model. Even a simple system requires complex differential equations to describe its behavior.

The issue for modeling is to synthesize a model that is simple enough to implement within these constraints but performs accurately enough to meet the performance requirements with a simple model which is insensitive to uncertainty. This simplification of the plant model is often referred to as model reduction. A more detailed treatment of modelling for a variety of physical system types can be found in [21]. In this work modelling is done with SimMechanics and thus all computational related problems where dealt by this application.

One technique for handling the model uncertainty that often occurs at high frequencies is to balance performance and robustness in the system through gain scheduling. A high gain means that the system will respond quickly to differences between the desired state and the actual state of the plant. At low frequencies where the plant is accurately modelled, this high gain results in high performance of the system. This region of operation is called the performance band. At high frequencies where the plant is not modelled accurately, the gain is lower. A low gain at high frequencies results in a larger error term between the measured output and the reference signal. This region is called the robustness band. In this region the feedback from the output is essentially ignored. This involves

setting the poles and zeros of the controller transfer function to achieve a filter. Between these two regions, performance and robustness, there is a transition region. In this region the controller does not perform well for either performance or robustness. The transition region cannot be made arbitrarily small because it depends on the number of poles and zeros of the transfer function. Adding terms to the transfer function increases the complexity of the control system. Thus, there is a trade-off between the simplicity of the model and the minimal size of the transition band. Gain scheduling is covered by [22]

5.1.2 The sensitivity function

The sensitivity function $S(s)$ that we will use is defined in the Laplace domain as:

$$S(s) \triangleq \frac{E(s)}{R(s) - d(s)}$$

where the symbol “ \triangleq ” is used to denote ”definition”. Thus the sensitivity function, $S(s)$, relates the external inputs, $R(s)$ and $d(s)$, to the feedback error $E(s)$ (fig. 5.2). Notice, however, that it does not take into account the effects caused by the noise, $N(s)$ (see [23] on pag. 34).

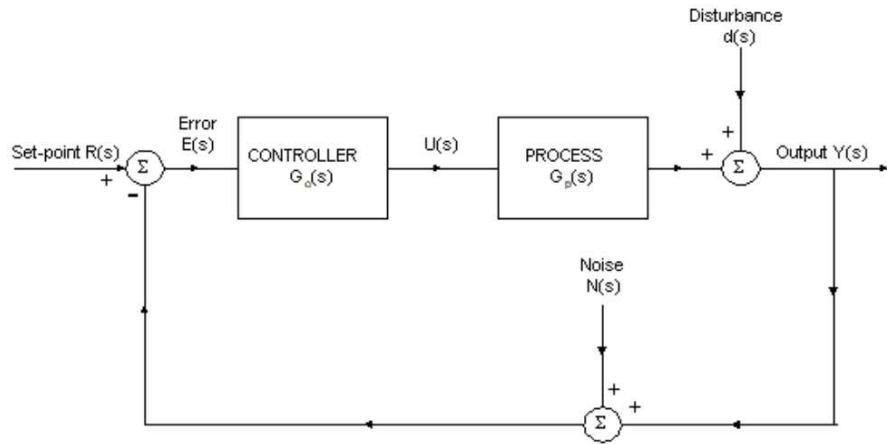


Figure 5.2: Schematic of conventional feedback control loop

5.1 Introduction to robust controllers

From the block diagram in fig. 5.2 neglecting $N(s)$, we can see that

$$E(s) = R(s) - Y(s) = R(s) - [G_P(s).U(s) + d(s)] \quad (5.1)$$

and $U(s) = G_c(s).E(s)$

$$\text{i.e. } E(s) = R(s) - G_c(s)G_P(s).E(s) - d(s)$$

$$\text{Rearranging, } E(s)[1 + G_cG_P(s)] = R(s) - d(s)$$

$$\text{Hence, } \frac{E(s)}{R(s) - d(s)} = \frac{1}{1 + G_c(s)G_P(s)}$$

$$\text{Since, } \frac{Y(s)}{d(s)} = \frac{1}{1 + G_c(s)G_P(s)} = \frac{1}{\frac{R(s)-d(s)}{E(s)}} = \frac{E(s)}{R(s) - d(s)}$$

it follows that

$$S(s) = \frac{Y(s)}{d(s)} = \frac{E(s)}{R(s) - d(s)} \quad (5.2)$$

therefore, the sensitivity function has an important role to play in judging the performance of the controller because it also describes the effects of the disturbance, $d(s)$, on the controlled output, $Y(s)$.

For the controller to achieve good disturbance rejection, $S(s)$ should be made as small as possible by an appropriate design for the controller, $G_c(s)$ ([24] and [25]).

However, most physical systems are “strictly proper”. In terms of their transfer-function repre-

sentation, this means that the denominator of the transfer function is always of higher order than the numerator. Thus,

$$\lim_{s \rightarrow \infty} G_c(s)G_P(s) = 0$$

In the frequency domain, this becomes

$$\lim_{w \rightarrow \infty} G_c(jw)G_P(jw) = 0$$

Hence,

$$\lim_{w \rightarrow \infty} |S(jw)| = \lim_{w \rightarrow \infty} \left| \frac{1}{1 + G_c(jw)G_P(jw)} \right|$$

therefore, $S(jw)$ has to be close to zero for ideal disturbance rejection, while, $S(jw)$ is one! What the results are telling us is that perfect control cannot be achieved over the whole frequency range some, basic concept on this mater can be seen in [23, 26]. The analysis shows that perfect control can only be achieved over a small range of frequencies, at the low frequency end of the frequency response. This subject is thoroughly developed in [24] and [25].

5.1.3 The complementary sensitivity function

The complementary sensitivity function is, as suggested by the name, defined as:

$$T(s) \triangleq 1 - S(s) \tag{5.3}$$

If there is no measurement noise, i.e. $N(s) = 0$, then since $S(s) = \frac{1}{1 + G_c(s)G_P(s)}$

$$T(s) = 1 - \frac{1}{1 + G_c(s)G_P(s)} = \frac{G_c(s)G_P(s)}{1 + G_c(s)G_P(s)} = \frac{Y(s)}{R(s)} \tag{5.4}$$

In this case, the complementary sensitivity function simply relates the controlled variable $Y(s)$ to the desired output, $R(s)$. Thus, it is clear that $T(s)$ should be as close as possible to 1 by an appropriate

5.1 Introduction to robust controllers

choice of the controller. Again, since most physical processes are strictly proper in the open-loop, i.e.

$$\lim_{s \rightarrow \infty} G_c(s)G_P(s) = 0$$

this means that, in the frequency domain,

$$\lim_{w \rightarrow \infty} |T(jw)| = \lim_{w \rightarrow \infty} \left| \frac{G_c(jw)G_P(jw)}{1 + G_c(jw)G_P(jw)} \right| = 0$$

As in the case of the sensitivity function, $S(jw)$, the desired value of the complementary sensitivity function, $T(jw)$, can be achieved only near low frequencies. This subject is thoroughly developed in [24] and [25].

5.1.4 The trade-off

When there is process noise, in terms of process inputs and outputs, $T(s)$ is also affected by $N(s)$. In this case, $T(s)$ has to be made small so as to reduce the influence of random inputs on system characteristics. In other words, we want $T(s) \approx 0$ or equivalently, $S(s) \approx 1$. Comparing this with the noise free situation where we require $T(s) \approx 1$ or $S(s) \approx 0$. This illustrates the compromise that often has to be made in control systems design: good set-point tracking and disturbance rejection has to be traded off against suppression of process noise (see [26] on pag. 203).

5.1.5 Weighted sensitivity

The sensitivity function S is a very good indicator of closed-loop performance, both for *SISO* and *MIMO* systems. The main advantage of considering S is that because we ideally want S small, it is sufficient to consider just its magnitude. Typical specifications in terms of S include:

1. Minimum bandwidth frequency.

2. Maximum tracking error at selected frequencies.
3. System type, or alternatively the maximum steady-state tracking error.
4. Shape of S over selected frequency ranges.
5. Maximum peak magnitude of S .

The peak specification prevents amplification of noise at high frequencies, and also introduces a margin of robustness. Mathematically, these specifications may be captured simply by an upper bound, $1/|w_P(s)|$, on the magnitude of S where $w_P(s)$ is a weight selected by the controller designer. The subscript P stands for performance since S is mainly used as a performance indicator, and the performance requirement becomes

$$|L(jw)| < 1/|w_P(jw)|, \forall w \quad (5.5)$$

$$\Leftrightarrow \|w_P(s)\| < 1, \forall w \Leftrightarrow \quad (5.6)$$

$$\boxed{\|w_P S\|_\infty < 1}$$

The last equivalence follows from the definition of the H_∞ norm, and in other words the performance requirement is that the H_∞ norm of the weighted sensitivity, $w_P S$, must be less than one.

5.1.6 Summary

From the above discussion, we can make the following observations:

- Both $S(s)$ and $T(s)$ have minimum values equal to 0 and maximum values equal to 1
- When there is no measurement noise,

5.2 H_2 and H_∞ optimal control

- For perfect disturbance rejection, $S(s) = 0$.
- For perfect set-point tracking, $T(s) = 1$.
- Perfect disturbance rejection also implies perfect set-point tracking, since $T(s) \triangleq 1 - S(s)$, i.e. perfect overall control. This can be illustrated by plotting both sensitivity and complementary sensitivity functions on the same graph, as shown in figure 5.3.

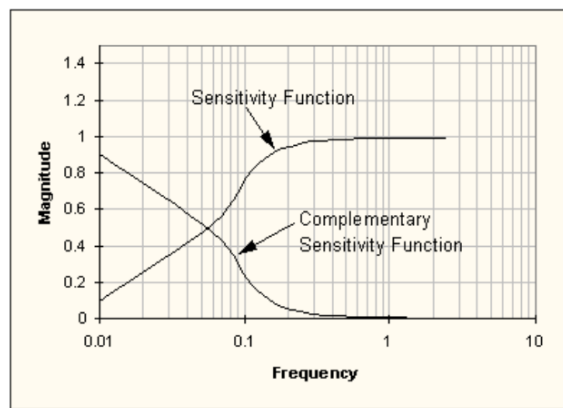


Figure 5.3: Sensitivity and Complementary Sensitivity functions of a closed-loop with a PI controller and a 1st-order system without delay

- When measurement noise is present
 - $T(s) \approx 0$ or equivalently, $S(s) \approx 1$ so as to reduce the influence of random inputs on system performance

5.2 H_2 and H_∞ optimal control

H_2 and H_∞ norms are frequently used as the cost measure in feedback optimization. This section describes interpretations of the norms as performance measures.

5.2.1 H_2 optimal control

The standard H_2 optimal control problem is to find a stabilizing controller K which minimizes

$$\|G(s)\|_2 = \sqrt{\frac{1}{2\pi} \int_{-\infty}^{+\infty} G(jw)G(jw)^T dw}; \quad (5.7)$$

For a particular problem, the generalized plant P will include the plant model, the interconnection structure, and the designer specified weighting functions. T is a partitioned system, obtained from P and the weighting functions: W_1, W_2, W_3 (see fig. 5.4)

$$G = \begin{bmatrix} W_1 s \\ (W_2/P)T \\ W_3 T \end{bmatrix} \quad (5.8)$$

By minimizing the H_2 norm, the output (or error) power of the generalized system, due to a unit intensity white noise input, is minimized; we are minimizing the root-mean-square (rms).

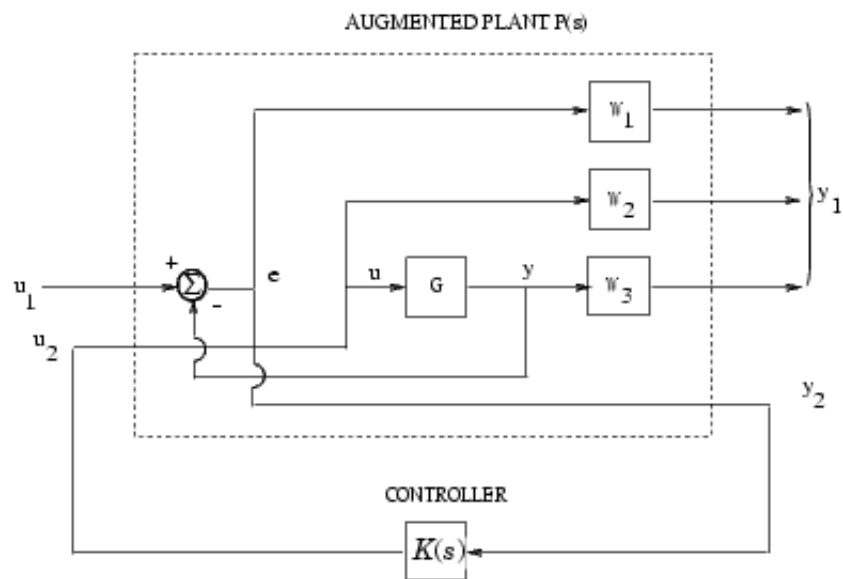


Figure 5.4: Weight functions

5.3 Pantograph control implementation

5.2.2 H_∞ optimal control

The standard H_∞ optimal control problem is to find all stabilizing controllers K which minimize

$$\|G_l(P, K)\|_\infty = \max_w \bar{\sigma}(F_l(P, K)(jw)) \quad (5.9)$$

We minimize the peak of the singular value of $F_l(P(jw), K(jw))$.

5.2.3 Robustness

In designing feedback controllers, we assume that the model, is exactly known. But in reality, system parameters such as weight, coefficients of viscous friction, resistance, capacitance, inductance, or other system constants, are often known inaccurately, or may change due to aging or other use-related factors. Some system characteristics are unknown or ignored, so there is an error between the real plant G and its nominal model, G_0 (see [22]). Now suppose that we have designed a stabilizing controller using the exact nominal plant model G_0 , so that the controlled system meets all given performance specifications for the nominal model. Will this controller, when used in conjunction with the real plant G , which may exhibit (often substantial) parameter variation about the assumed nominal values, still produce a stable system? Will the performance specifications still be achieved in the presence of these variations in system parameters? If the answers to these questions are in the affirmative, then we say that we have designed a robust controller, i.e. the resulting feedback control system is one for which the stability and performance properties are robust with respect to the uncertainties.

5.3 Pantograph control implementation

In this section the controller implementation in Simulink[®] is presented. Implementation is done by means of a closed-loop strategy that can be seen in fig. 5.5. The model of the control system presented

in the previous figure is of a pantograph / catenary system. Model disturbance and sensor noise is included in the control ring. The reference signal introduced in the system is a constant value that depends on rail norms and other specifications. The control theory developed produces the controller in state space representation, which is defined as $K(s)$.

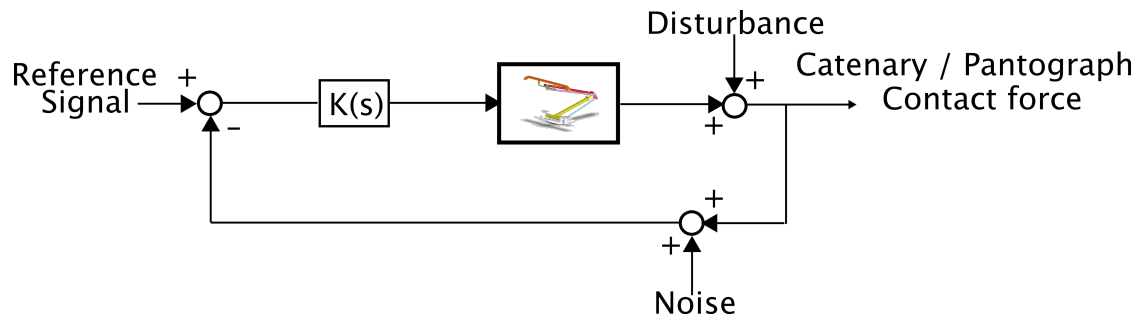


Figure 5.5: Pantograph control closed loop representation

Chapter 6

Results and discussion

6.1 Pantograph type overview

In this section five pantograph models will be studied. The Type 1 pantograph model is the base study model, it is very similar to the *SNCF* pantograph which is the high speed pantograph in circulation in France with the *TGV*. This pantograph is composed by mass, joints and passive elements. It has two degrees of freedom which are represented in fig. 6.1. The motion of the pantograph is upwards and downwards depending on the force sensed by the registration strip (F_c), thus the equation of static equilibrium applied in stationary conditions is valid and used for calibration. The force F_c is the force that the catenary exerts on the registration strip.

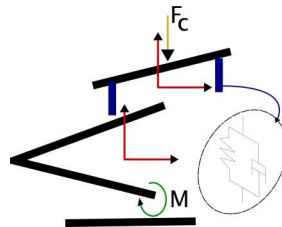


Figure 6.1: Pantograph with one actuator and with springs and dampers present in the registration strip (Type 1)

In this chapter the catenary perturbation will be modeled with a periodic sine function of 2 Hz and

6.2 Pantograph type overview

20 Hz or a step function. The amplitude of the perturbation signals are the same and of magnitude of 10 cm. These settings apply to all experiments. The first experiments are for the Type 1 and type 3 pantographs, and all types of perturbations were used. From the first experiments two controller settings were developed focusing robustness with poor performance and a second controller with better performance but inferior robustness to model change. The second set of experiments tend to focus on passive element presence. These sets of experiments were also made with the Type 1 and Type3 models. The third set of experiments was dedicated to study the model behavior due to physical parameter changes. The fourth set of experiments was to evaluate the performance of a double actuated pantograph. The fifth set of experiments was to test the Type 5 pantograph with a periodic perturbation function and to understand isolated controller for top actuation, and combined lower and top actuation. All sets of tests use for control a PID controller or a robust controller. The final set of experiments confronts the model obtained with the experimental results.

6.2 Pantograph type overview

The Type 2 pantograph, is a representative of a standard pantograph which is used in normal train lines (CP or Fertagus transportation companies), to study their behavior and to suggest the best physical implementation in terms of springs, dampers or actuated elements and to study the influence in system dynamics. In the preceding chapter, robust controllers were developed and thoroughly analyzed. With these results, a better understanding was gained over the controller limitations and potentialities that can be used with high speed trains. The modelled registration strip, is attached to the stabilization arm as can be seen in fig. 6.2 with no passive elements.

The Type 3 model purpose is to better simulate the motion of the catenary cable on top of the

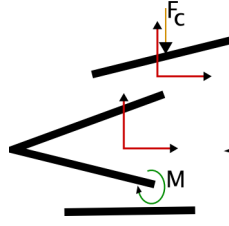


Figure 6.2: One actuator pantograph with fixed registration strip (Type 2)

registration strip. Instead of having a fixed force applied in the center of the pantograph registration strip, we have a moving force that slides along the registration strip frame, thus simulating better the effects of catenary dynamics over the pantograph. The sliding force that has its own frequency, changes the dynamics of the coupled system. In other terms, the contact force F_c in an open loop configuration will have higher frequency due to the sliding force. A representation of this model can be seen in fig. 6.3, which has only one actuator present in the joint that connects the base to the lower arm.

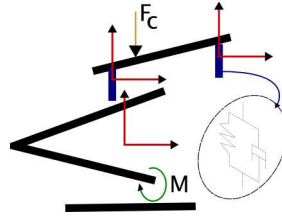


Figure 6.3: One actuator pantograph with 2 *DOF* registration strip (Type 3)

The Type 4 and Type 5 pantograph models (see fig. 6.4) are models that include control. Introducing active control to the registration strip is the main objective here. The Type 4 model has in the contact interface only one degree of freedom, the Type 5 model has a sliding catenary cable on the registration strip. These models include actuators which are placed in the joint that connects the base to lower arm, and the joint that connects the stabilization arm to the registration strip.

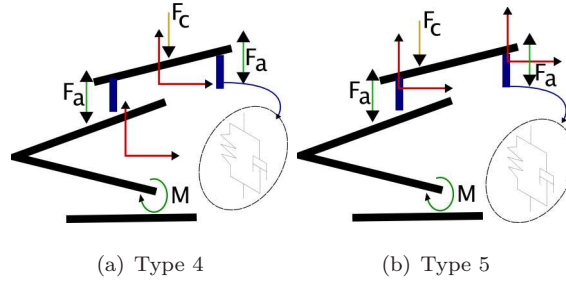


Figure 6.4: The Type 4 and Type 5 pantograph models

6.3 Linearization

The process of obtaining a linear model from the nonlinear *SimMechanics*[®] model gets more complex, as the contact interface between registration strip and catenary cable is more accurately modelled. Moreover if the model gets too “heavy”, having many degrees of freedom or having many joints, obtaining a linear model is harder to achieve. Another important issue is to guarantee that the system will work close to the nominal conditions. Instead of using traditional *ARX* or *ARMAX* identification methods, an indirect use of these tools was preferred, thus the usage of the linearization package in *Simulink*[®]. *SimMechanics*[®] provides linearization trimming. Because the system we wish to control is a coupled system and uses two different environments thus not being natively in *SimMechanics*[®], the trimming method isn’t a useful solution. Instead of that approach, a global linearization of the *Simulink*[®] model is used, resorting to the *Control Toolbox*. The linearization utility focuses mainly on two basic informations: the operating conditions of the model and the linearization method used. The operating point, as described in chapter 5, is relative to the nominal function of the pantograph, which is assumed to be the initial configuration of the coupled system. The number of states changes, depending on: the type of model, the operating point searching tool and the linearization method. Some linear models obtained weren’t good enough or had too many states. A good example of state correspondence with the nonlinear model was found in the Type 1 system where we have four states

that relate directly with two rotation joints of the pantograph, one translational (1 DOF translation joint) joint belonging to the pantograph also and finally one translational joint belonging to the catenary system. Here we can see that the states relate well to the physical system. Unfortunately other state configurations were obtained an example of this was to have more states than needed, these linear models were classified as bad linear model candidates.

6.3.1 Linearization of the nonlinear model

The operating point is defined by the initial position and orientation of the pantograph. The expected dimension of the system is a *MISO* system, two inputs one output system, where in this case one of the input signals is a perturbation. Thus, the system we are analyzing is in fact a *SISO* system (eq. 6.1 and eq. 6.2), with perturbation added to it and therefore all the traditional *SISO* theory is applied directly.

$$\dot{x} = \begin{bmatrix} 0 & 1 & 0 & 0 \\ -1313 & -5.6 & -127.3 & 33.58 \\ 0 & 0 & 0 & 1 \\ 150.1 & 0.5427 & -7.1 & -11.07 \end{bmatrix} x + \begin{bmatrix} 0 & 0 \\ -0.02087 & 52.6 \\ 0 & 0 \\ 0.0062 & 0 \end{bmatrix} u \quad (6.1)$$

$$y = \begin{bmatrix} -500 & -10 & -1676 & -33.52 \end{bmatrix} x + \begin{bmatrix} 0 \\ 500 \end{bmatrix} u \quad (6.2)$$

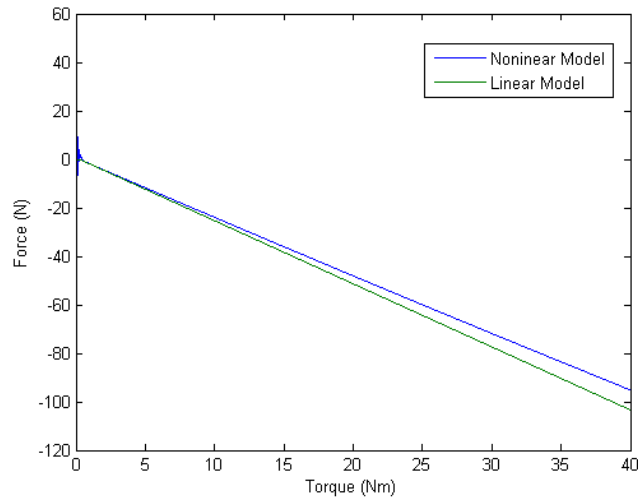
The system can be seen in transfer function where G_1 is the relation between joint torque (Nm) and catenary force (N) and G_2 is the relation between catenary perturbation (m) and catenary force (N), the transfer function representation of the system can be seen in eq. 6.3.

$$G_1 = \frac{-0.5702s^2 - 188s - 7973}{s^4 + 16.68s^3 + 1365s^2 + 9611s + 28470} \quad (6.3)$$

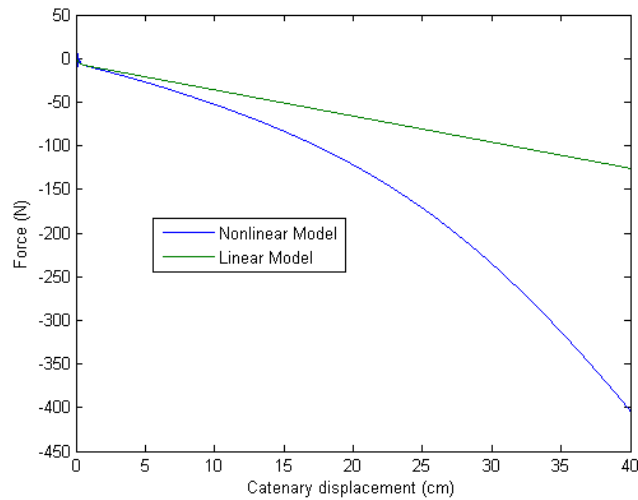
$$G_2 = \frac{500s^4 + 7812s^3 + 6.492e05s^2 + 4.198e06s + 8.094e05}{s^4 + 16.68s^3 + 1365s^2 + 9611s + 28470}$$

6.3 Linearization

The Type 1 model will be the reference model used, and the linearized system can be viewed in eq. 6.1. As can be seen from fig. 6.5, which is the model validation figure. The linear model obtained approximates the nonlinear system for catenary displacements lower than 0.1m. Above this value it will be considered that the linear system obtained isn't suited. Model validation was based in torque variation with no perturbation (see fig. 6.5a) and perturbation variation with no torque (see fig. 6.5b).



(a) Torque



(b) Catenary displacement

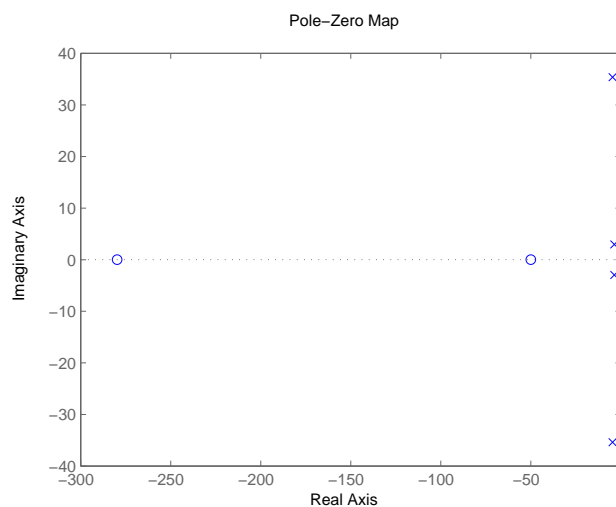
Figure 6.5: Model validation: input variation

The pole zero map of G_1 can be observed in fig. 6.6 and the respective values in table 6.1. Some

systems obtained by this tool were numerically badly conditioned, and of high order, thus not being suitable candidates for linear pantograph models. It was found by experience that block by block linearization, with default options, to be the best solution for obtaining the linear system model; normally numeric perturbation is best suited, but because *SimMechanics*[®] is used, there can be great influences in having better results with block by block linearization. The default settings also include a gradient descent with elimination method (see [27]) for default operating point method. Also better results were obtained by letting the system stabilize (equilibrium) and then take a snapshot of the model for linearization. This method proved to give great approximation between nonlinear and linear models, the only problem was that the state space system had many states and was numerically badly conditioned.

Poles	Zeros
-4.6496 +35.3892i	-279.72
-4.6496 -35.3892i	-49.9885
-3.6904 + 2.9543i	
-3.6904 - 2.9543i	

Table 6.1: Poles and Zeros


Figure 6.6: Pole Zero Map: Torque in joint vs Force in catenary (G_1)

6.3 Linearization

To correctly introduce the linear model, pole-zero maps, controllability and observability analysis had to be done. In fig. 6.6 and eq. 6.3 we can see that the system is stable in an open-loop configuration alike the nonlinear model, and that it is observable and controllable. We can see that $rank(C) = 4$ and that $rank(O) = 4$, this means the system is observable and controllable (see 5).

Controllability matrix

$$C = \begin{bmatrix} 0 & -0.0208 & 0.3255 & 22.0641 \\ -0.0208 & 0.3255 & 22.0641 & -611.9188 \\ 0 & 0.0062 & -0.0801 & -2.1098 \\ 0.0062 & -0.0801 & -2.1098 & 84.7572 \end{bmatrix} \quad (6.4)$$

Observability matrix

$$O = \begin{bmatrix} -500 & -10 & -1675.9778 & -33.5196 \\ 8104.4101 & -462.1093 & 1517.3624 & -1640.6978 \\ 360743.1467 & 9805.6851 & 70788.1001 & 4163.1773 \\ -12255792.3557 & 308038.4084 & -1278405.276 & 353978.097 \end{bmatrix} \quad (6.5)$$

6.3.2 Conclusions from linearization

In this section, it was learned that the linear systems work in a small region. From table 6.2 is shown that the catenary displacement varies about 3 cm. From this point it will be considered a maximum displacement of 10 cm which is a little out of the functioning zone but will help to test model robustness. The type one model as expected is controllable, observable and well conditioned and thus proper for deriving a robust controller. Unfortunately it wasn't possible to use other methods for model linearization other than *block by block linearization* because of the state space badly conditioned matrices.

Many types of linearization techniques were tried, but with no success: all the linear models obtained had very poor resemblances with the nonlinear model. The approximated linear model can

be seen in fig. 6.7b which is of Type 1. Figure 6.7a shows a more complex linear model but no correct state space equations were found thus the system hasn't represented correctly. The main problem was the catenary motion which slides along the registration strip frame.

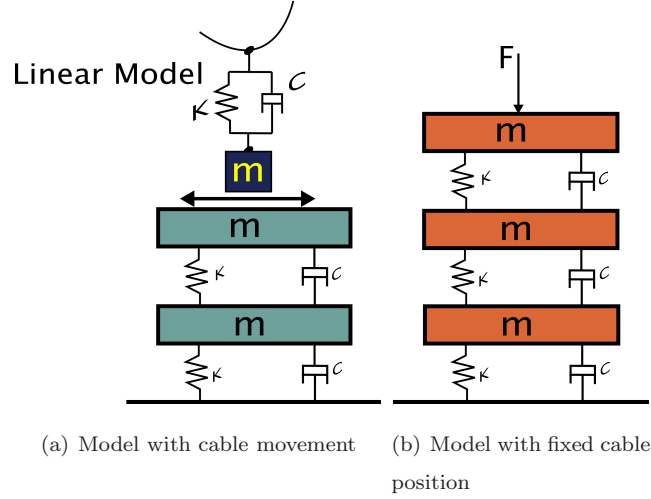


Figure 6.7: Pantograph linear models

6.4 Problem statement

From the previous sections it is possible to see that there are big force variations in the contact interface, and that there are some differences between the models used in section 6.5 and the models formulated in this work. From section 6.6 it was seen that the system naturally takes time to respond to step perturbations, and for a sine perturbation no constant force value is achieved, moreover it is oscillating in magnitude with the varying displacement of the catenary. From the force readings presented in section 6.5 one can see that the frequencies assumed are very different from what is expected in reality. In real applications it's possible to have a really intense varying force (due to wind and catenary mode vibrations) giving large magnitudes with increase frequencies up to 20 Hz (see [8] and [1] for an example of sine perturbation as catenary). In this case, it is desired to attenuate the force magnitude (to filter the catenary effect) over the pantograph. Some interesting

6.5 Experimental results and motivation

tests were made with the Type 1 and Type 2 models, as can be seen in fig 6.12 and 6.13, that the force magnitude sensed by the pantograph is catenary frequency dependent. This means that to balance the high frequencies, not only will the system need to react faster, but also will have to deal with bigger force deviating amplitudes offered by the system inertia.

Because the pantograph will be used for human transportation lines, safety and reliability is an important factor. The objective of this work is to present a reliable robust system for train implementation. Industrial applications normally tend to use standard *PID* systems due to simplicity. The problem of using robust controllers is normally on the order of the controller, that is in general of higher order than normal *PID* solutions. This means that they are harder to configure and to design. In order for the control scheme to be valid, some important criteria will have to be set: the controller has to withstand model parameter variations (mass, springs and dampers), and other model uncertainties. Instead of deriving uncertainty directly from the model parameters, and designing a controller that withstands the desired robustness and performance requirements, the approach followed deals with uncertainty in terms of controller actuating frequencies. This means that on specific frequencies (normally high frequencies) the controller will have low action and on working frequencies it will have high action, thus having a bigger margin of stability. The problem of this type of controller is that not always there will be a solution that minimizes the energy and therefore not having simultaneous robustness and performance.

6.5 Experimental results and motivation

To motivate the study in this chapter, experimental results from *SNCF* train circulation were used. These results are presented in fig. 6.8, which can be found in the *SNCF* training session manuals

[28].

In order to compare the achieved results, two sources were used offering experimental data which will be useful for model comparison and control validation. The experimental data is presented in fig. 6.8 and fig. 6.9, which come from different sources. Table 6.2 is obtained from fig. 6.8 where the data in this table serves simply to get an idea of the force magnitude in the contact interface and the registration strip displacement maximum values

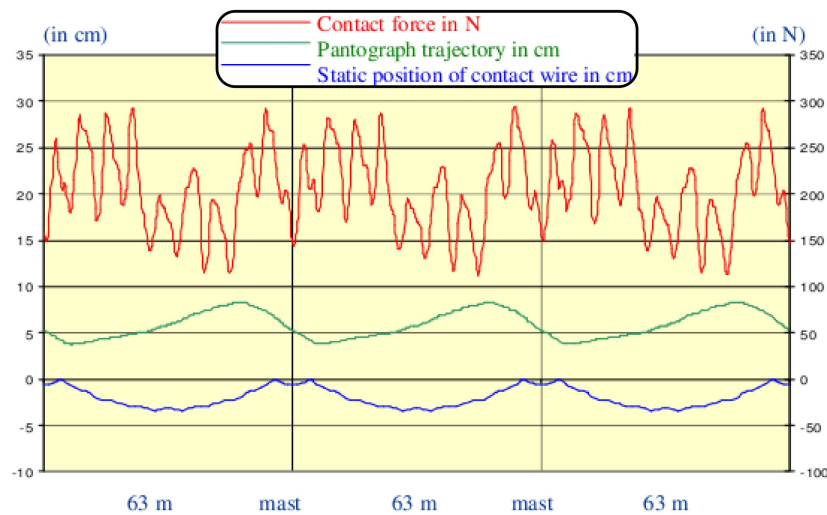


Figure 6.8: Training Session in High Speed Systems

From fig. 6.8 and the data presented in table 6.2 and table 6.3, a very important conclusion can be undertaken. The contact force varies greatly in magnitude over time. It can change about $190N$ of contact force, this value of variation can represent a value as large as the calibration force values in nominal conditions. Although today this variation value is acceptable, in the future these variations will not be tolerated. From the same tables, the pantograph lift and descent motion can be analyzed. The maximum variation in height can be of $3cm$ which is a very low value. This information can be very tricky because it can be relative to a small portion of the track meaning that in other segments bigger variations could be expected. An example is a tunnel where the pantograph and cable system

6.5 Experimental results and motivation

$y_{cat}(cm)$	$y_{pant}(cm)$	$F(N)$
0	4	170
-3,8	6	150
0	6	230
0	4	210
-3,8	6	170
-2,2	7,5	110
0	6	300
0	4	255
-3,8	5,8	180
-2	8	225
0	6	240

Table 6.2: Global *SNCF* pantograph experimental results

Results		
$y_{cat_{Ref}}$	0	cm
Δmax_{cat}	3,8	cm
$y_{pant_{Ref}}$	5	cm
Δmax_{pant}	3	cm
ΔF	190	N

Table 6.3: Experimental results highlights

is lowered compared to its nominal position. Still, a $3cm$ variation corresponds to a very small change in height. With these results, considering a catenary displacement of $10cm$ is very ambitious and a good robust performance test. Furthermore, from fig. 6.9 it's possible to see that the pantograph besides the noise has a high functioning frequency due to catenary 2-D motion along the registrations strip frame.

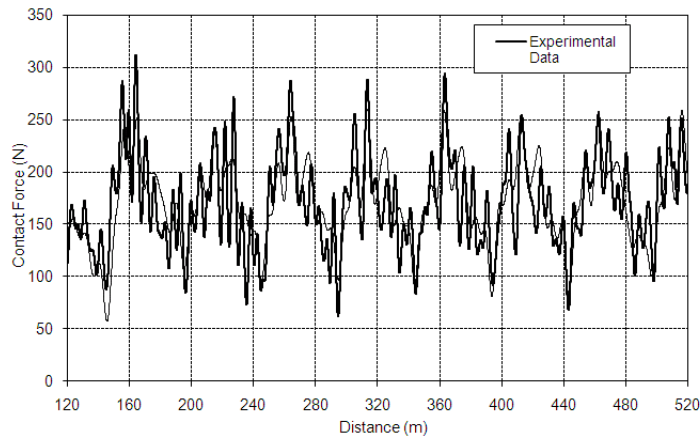


Figure 6.9: *SNCF* experimental results

6.6 Pantograph and catenary nonlinear model attributes

In chapter 4 a nonlinear model of the pantograph and the catenary was presented, which can be seen in fig. 4.1 and fig. 4.10. Here also five models were introduced, where the differences between them were the passive elements that are attached to the registration strip and the actuator inputs.

In this section we are interested in studying the open-loop behavior of each model. Before any type of analysis, some questions about modelling the pantograph have to be pointed out. What is the influence of passive elements on the contact interface? What are the problems that are introduced by passive elements in obtaining a nominal system condition when using a coupled system (pantograph + catenary)?

The Type 1 model presented is very similar to a real pantograph but except for the consideration of catenary movement along the registration strip frame. In this case no movement is considered, and thus the force sensed by the registration strip center is the same sensed by the catenary. An illustration of the forces involved in the contact interface is presented in fig. 6.10.

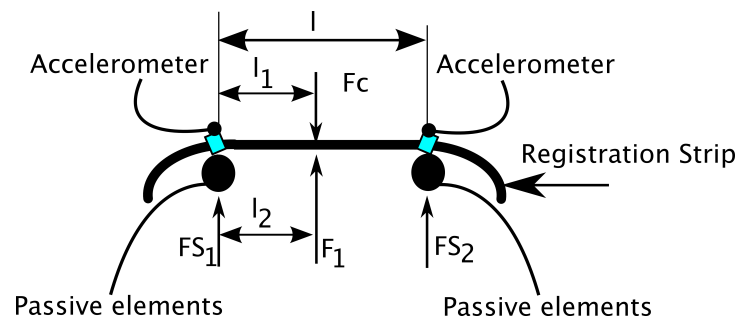


Figure 6.10: Free body diagram of Type 1 registration strip

To respond to these questions, instead of analyzing all models, only relevant models will be discussed in each section. In this section special aim will be given to the Type 1, the Type 2 and the Type 3 models. We will start this study by the Type 1 model. This model has the following charac-

6.6 Pantograph and catenary nonlinear model attributes

teristics: it is actuated in the joint that connects the base to the lower arm, it has passive elements in the registration strip, there is no relative movement between left and right passive element, and the catenary is considered to be centered in the registration strip frame. The model can be seen in fig. 6.1, where in chapter 4 was explained why in this case the contact force is given by the catenary system.

The contact force rises when a displacement is applied over the registration strip. The pantograph takes time to react by it self but it will naturally compensate the force addition with it's own vertical displacement, to be in equilibrium conditions (see fig. 6.10, and see fig. 6.11).

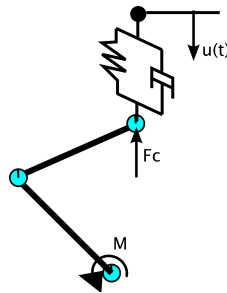
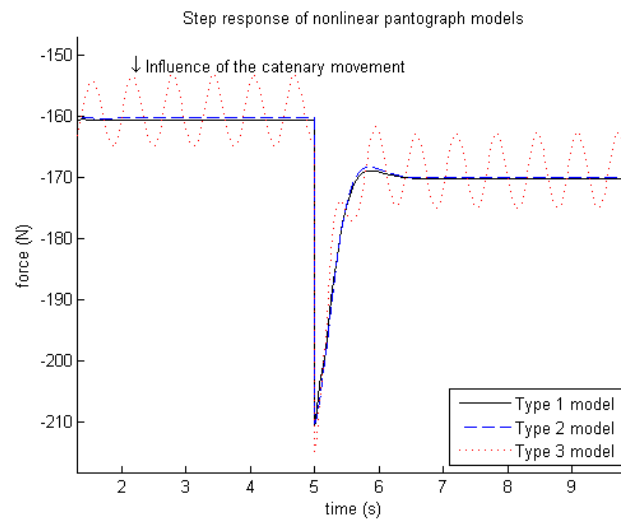


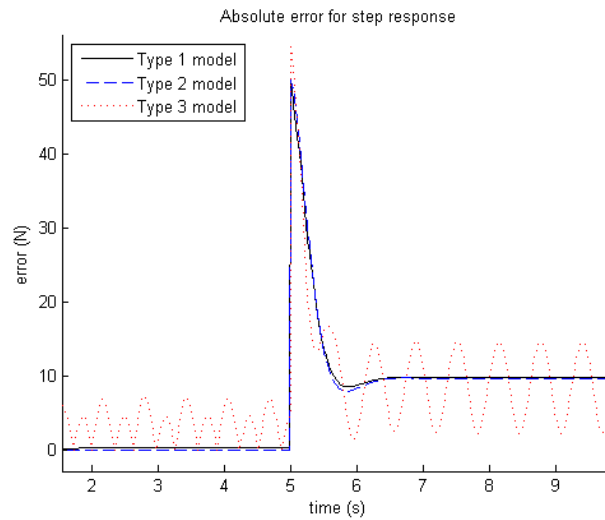
Figure 6.11: Pantograph model representation

The Type 1 model is the base model, meaning that all state space controllers designed will be based on the linear system derived from this model. In chapter 4, it was explained that in order to simulate the catenary effect on the pantograph, the position of the spring damper system would have to be changed to produce an increase or decrease of contact force. This perturbation will be the target of discussion due to it's direct influence on the static contact force measure. The first type of perturbation studied was a step input displacement on the catenary of 0.1 meters. The results are presented in fig. 6.12.

Changing the step perturbation to a sine input signal to the catenary position, with a 2 Hz frequency and an amplitude of 0.1 meters of catenary displacement, offers interesting results which



(a) Force



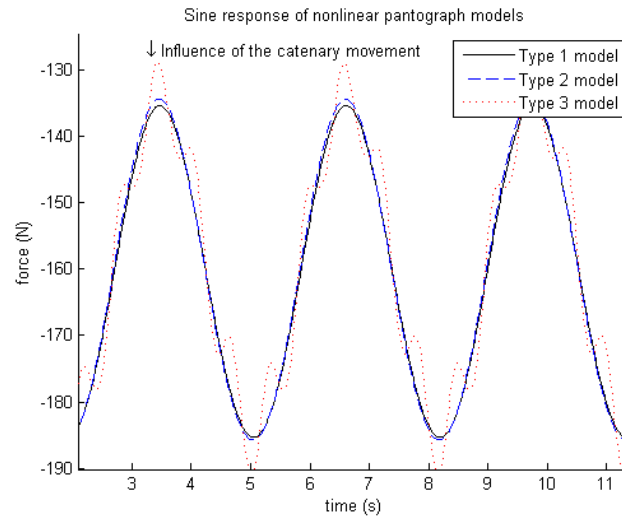
(b) Absolute error

Figure 6.12: Pantograph open-loop with catenary step perturbation

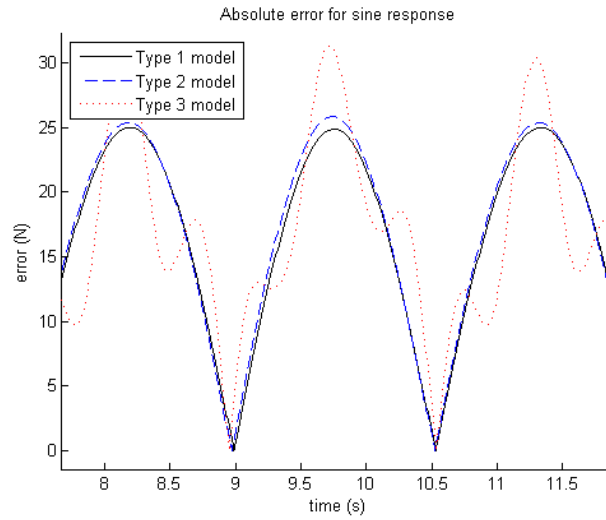
are presented in fig. 6.13.

6.6.1 Conclusions from open-loop modelling

From the presented results, it is possible to view the difference between the model in *SimMechanics*[®] and the results presented in the experimental data. Although the working perturbation frequency is different in both models (considering the two models presented in the previous section as one type of



(a) Force



(b) Absolute error

Figure 6.13: Pantograph open-loop with catenary sine perturbation

model). This means that the coupled system is still far from the real dynamics of coupled pantograph catenary system. Other information can be understood from the open-loop system, the analyzed models are stable and they have an offset relative to the target working contact force. The reference contact force was assumed of 160.3 N, this target is different from the experimental data. An idea of this value can be seen in fig. 6.8 as more or less the mean value.

6.6.2 Model comparison with experimental results

The pantograph was modeled without any experimental data information and therefore the results presented aren't tuned for the experimental data. Many information was assumed and may not represent the real experimental simulation. In fig. 6.14 and 6.15 it is shown that the models don't approximate the experimental data. The frequency presented of 2 Hz follows from the knowledge of the assumed low frequency catenary influence. Assuming a train velocity of 350 Km/h and a catenary span of 60 m it was concluded that the low frequency would be of 1.76 Hz approximately 2 Hz. Experimental results contradict this assumption, for low frequencies it was verified that a 7 Hz perturbation would approximate more the experimental data. Not only in frequency there are differences but also in force amplitude, this happens because the catenary model constants are incorrect (spring and damper).

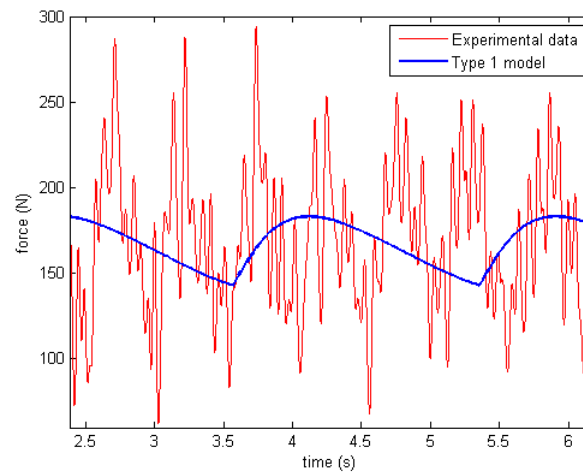


Figure 6.14: Type 1, 2Hz, with 10 cm amplitude, sinusoidal catenary perturbation

6.7 Model sensitivity to parameter changes

The model by itself contains physical uncertainties. Varying the magnitude of mass, spring and damper elements can change model behavior. Admitting physical property uncertainties at a maximum of 30%,

6.7 Model sensitivity to parameter changes

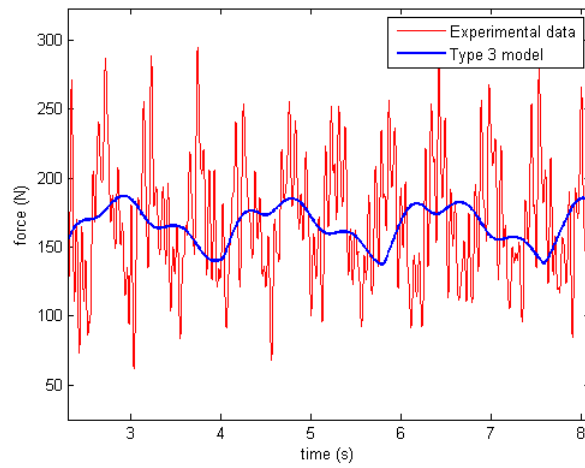


Figure 6.15: Type 3, 2Hz, with 10 cm amplitude, sinusoidal catenary perturbation

it is desired to see what happens to the system poles and zeros, when these changes take effect. In this section only the Type 1 model will be studied. In fig. 6.16, fig. 6.17 and fig. 6.18 are presented some pole-zero maps of the Type 1 model, but with one different parameter value change per graph.

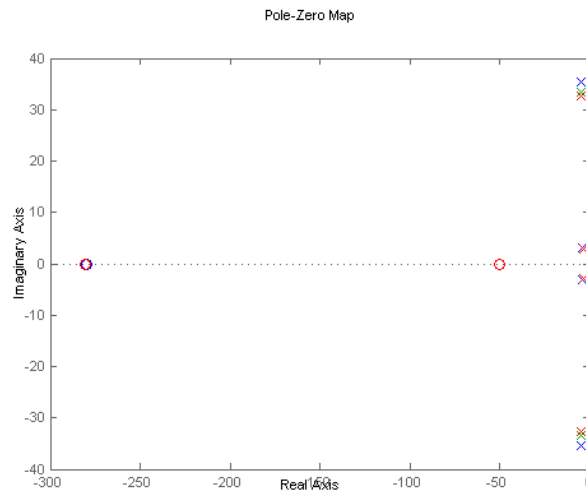


Figure 6.16: Model mass parameter and pole-zero map

As seen in fig. 6.16, mass variation has a heavy effect on the linear model poles, bringing them closer or not to the origin. Adding mass to system approximates the poles to the origin, giving higher rigidity to the system, in an open-loop configuration. From the zero positioning (which in fig.

6.16 is represented by a circle), it is detected that it moves towards the origin with the increase of mass, thus making the system more sensitive to perturbations and potentially unstable in closed-loop configuration for the same controller proportional gain.

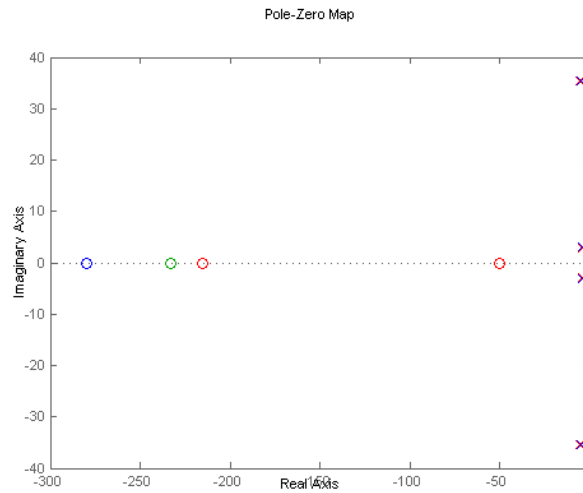


Figure 6.17: Model spring parameter and pole-zero map

From the analysis of fig. 6.18, and by simulation experience, it can be said that there are two very important elements to consider, registration strip mass and attached dampers, the last one will condition the study in the next sections. The existence of damper elements directly affects active element performance, which will be explained further on. The mass variation in the registration strip can condition the effectiveness of the passive elements and limit their capacity to absorb the catenary dynamics. Spring analysis was also done and is presented in fig. 6.18.

6.8 Closed-loop pantograph analysis

To solve the problem of the open-loop configuration, it's important to understand the problem in hands. The base pantograph in study is the Type 1 pantograph model and it has passive elements attached to the lower arm and the registration strip. A question that has to be made is that what

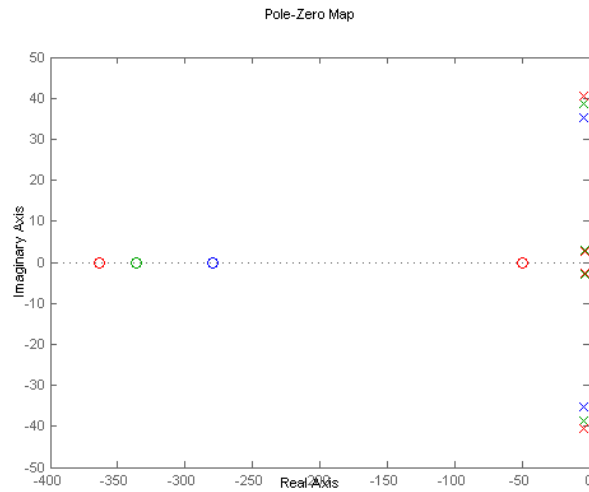


Figure 6.18: Model damper parameter pole-zero map

influence do model elements have in control? A bad configuration of passive elements placed in the pantograph can limit severely the controller performance. This will be demonstrated in this section. There is no point in maintaining passive elements in control when they are not contributing for better performance.

With the objective of obtaining a constant force at the contact interface, two types of catenary perturbations will be used, a step and sine perturbation displacement of the catenary. The closed-loop step response is shown in fig. 6.23. A special remark has to be said at this point, although in this work the second perturbation is called sine perturbation displacement, it is in fact a $|\sin(z)|$ form function, it's just called sine perturbation for simplicity.

6.8.1 Controller development

All controller development will be based upon the Type 1 model. The first step in the creation of a robust controller is the definition of the output and input weighting functions.

Weighting functions

The weighting functions are chosen by the controller designer. Unfortunately it's not possible to achieve easily a perfect weighting function combination, some configurations can produce low performance controllers, others will produce high performance with no change in robustness. The weighting functions obtained were used both on H_∞ and H_2 controllers. Two sets of weighting functions are used, the first is a more conservative approach, the second is a more aggressive controller but with the possibility of robustness reduction. Many orders for the weighting functions were tested and for simplicity a first order transfer function was used (see eq. 6.6)

$$w_1 = \left(\frac{w_0}{\tau s + 1}\right)^n, w_2 = 0.1, w_3 = 10^{-3} \quad (6.6)$$

$$w_0 = 10; \tau = 50; n = 1 \quad (6.7)$$

Where the w_3 is the actuator effort weighting function. Alike standard *PID* controllers, robust controllers have to be tuned. There are essentially two important weighting functions which are the output and input plant error weights, these parameters were obtained with trial and error, an example of the process can be seen in fig. 6.19. Here we can see the evolution of changing the τ parameter in a first order w_1 weighting function.

Uncertainty model and controller development

To make a preliminary study of model robustness, a family of systems similar to the Type 1 model are derived and thus creating an uncertainty block. This can be seen in fig. 6.20, which is a frequency response for the nominal system, with 10 samples of uncertain system and the uncertainty. With the help of the *Robust Control Toolbox* these elements are studied to understand the controller robustness due to plant variation. A remark has to be done here, instead of analyzing the system from it's basic

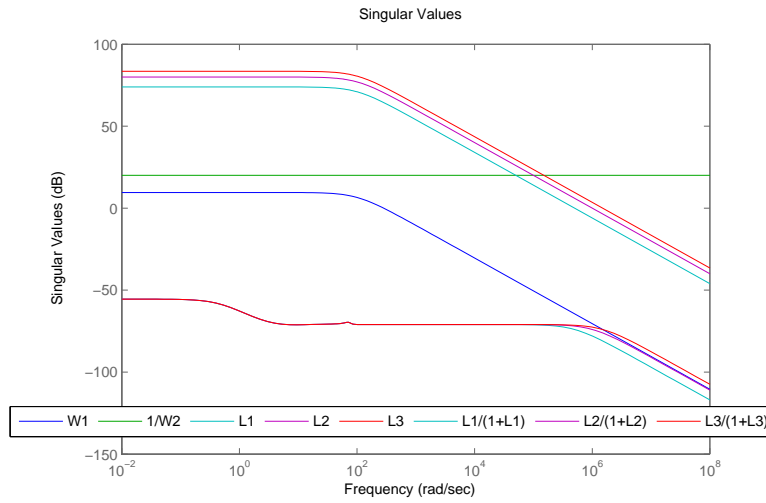


Figure 6.19: Testing w_1 : Loop shaping

properties and deriving model uncertainty based on mass, damper, spring or other property parameters change (which is done in [22]), uncertainty is placed in the model natural frequencies. Changing this alters the systems transfer function and thus is also proper to study controller robustness to model uncertainty. A result of this is that there may not be any relation between model parameters and uncertainty. Both methods were studied.

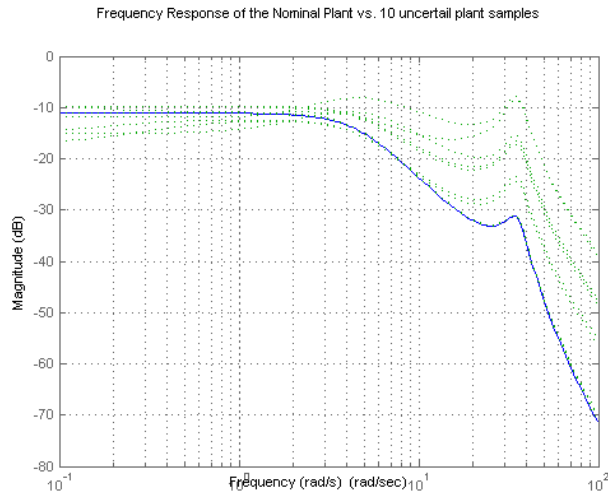


Figure 6.20: Multiple models based on Type 1 model

The controller was obtained with the help of the *Robust Control Toolbox* in *Matlab* and the ex-

pressions is as follows. The controller function used is presented in eq. 6.8, where k is the controller developed to be placed in the closed-loop (see [29] for more details).

$$[k] = \text{hinfsyn}(\text{plant}_i c, 1, 1, 'Display', 'on', 'Tolgam', 1e-3); \quad (6.8)$$

Where K is the closed-loop controller. An H_∞ control law has been designed which achieves an infinity norm of 0.9066 for the interconnection structure, the interconnection structure is a closed-loop representation of the controlled system in a special Matlab variable. The H_∞ controller K the state space representation of:

$$A = \begin{bmatrix} -4545 & 1122 & 6655 & 5108 & 1.6e+004 \\ 146 & -27.5 & -172.9 & -132 & -398 \\ 465.6 & -144.5 & -685 & -525.1 & -1639 \\ 278 & -70.68 & -396.6 & -309.6 & -973 \\ -1494 & 379.9 & 2183 & 1677 & 5248 \end{bmatrix} \quad (6.9)$$

$$B = \begin{bmatrix} -0.003671 \\ 0.001235 \\ 0.005232 \\ 0.003393 \\ 0.01355 \end{bmatrix} \quad (6.10)$$

$$C = \begin{bmatrix} -1.359 \times 10^5 & 3.503 \times 10^4 & 1.993 \times 10^5 & 1.531 \times 10^5 & 4.799 \times 10^5 \end{bmatrix} \quad (6.11)$$

$$D = \begin{bmatrix} 0 \end{bmatrix} \quad (6.12)$$

The loop shaping process was used to confirm if the system could achieve the performance levels desired, it was observed that depending on the controller designer demands for control the infinity norm (or the alternate H_2 method) could not produce a controller that delivered the controller performance and robustness desired at the same time. The problem was the transition zone. To solve this, higher order weighting functions were used but this often resulted in low performance controllers. In general the robust toolbox produced systems which respects Doyle's stability criteria or the small gain theorem

6.8 Closed-loop pantograph analysis

(see [26] or [25]). The closed-loop singular value plot that in a *SISO* system corresponds to the Bode's gain plot which can be seen in fig. 6.21. From fig. 6.21 e we can see that the desired controller doesn't fit totally the magnitude and working frequencies desired. More studies have to be done on efficient robust controller tuning for better and fast loop shaping with a smaller transition zone.

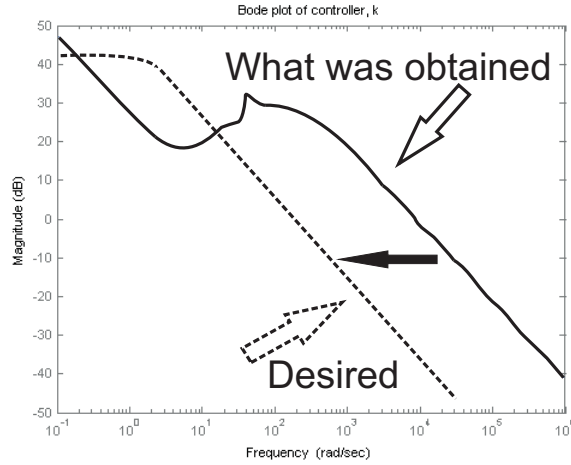


Figure 6.21: Robust Controller gain plot

The methodology to obtain an H_2 robust controller is the same with the only difference in the Matlab expression used. The controller obtained had the same global characteristics as the H_∞ with one difference which was having less problems converging to a solution, this is explained in chapter 5. The systems behavior to the controller is approximately the same as H_∞ controller, thus showing that the major differences occur in the mathematical formulation.

$$[k, g, gamma, info] = h2syn(plant_c, 1, 1); \quad (6.13)$$

The *PID* controller used was tuned based on trial and error, the weighting gains obtained are respectively: $P = 15$, $I = 3$, $D = .1$

The controller above is relative to the lower joint. For the upper joint, which are the vertical translation joints that support the registration strip another set of *PID* controller gains where used:

$$P = 15, \quad I = 3, \quad D = .1$$

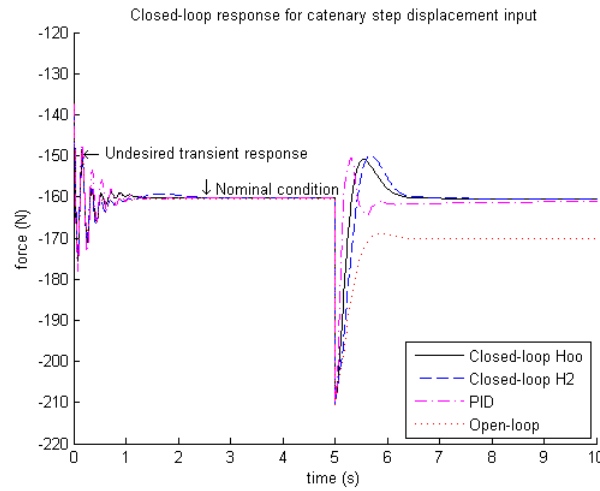


Figure 6.22: Type 1 with 2Hz sine perturbation controller comparisons

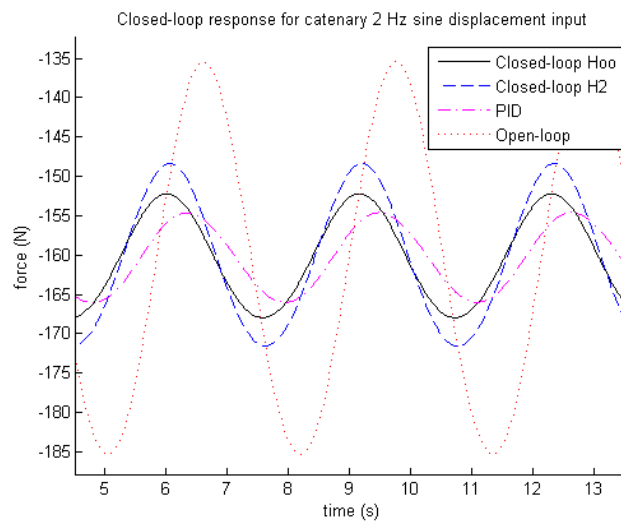


Figure 6.23: Type 1 step perturbation controller comparisons

6.8.2 Results

The results presented show that all controllers developed can perform well under a step response considering that it's only meant to work with this perturbation, if the step were to repeat itself frequently like for example a periodic function the controller performance would be quite different and to please both types of perturbations can be quite complex to obtain with robustness. The next

6.8 Closed-loop pantograph analysis

test made is a sine perturbation input displacement to the catenary (see fig. 6.24), the amplitude remains the same as the step test, which is of 0.1 meters. The frequency in this test is of $2Hz$ and of $20Hz$, so it is expected that the results for the $20Hz$ frequency perturbation with the same controller to be poor. The explanation of this phenomena is the target of the next paragraphs.

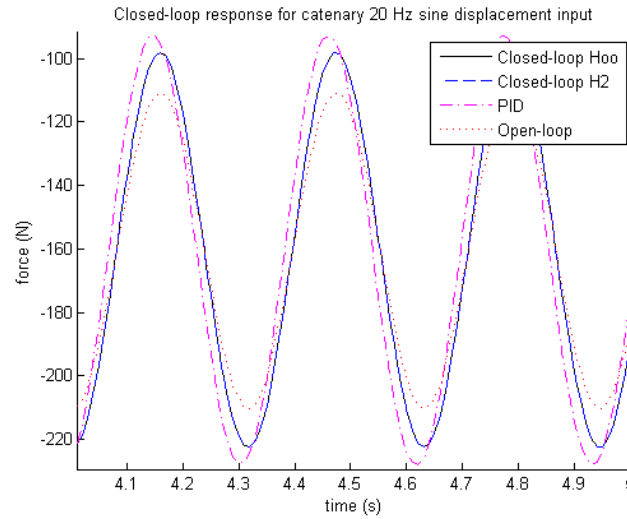


Figure 6.24: Type 1 with $20Hz$ sine perturbation controller comparisons

The robust controllers used here have the weighting functions which were already defined previously.

From the results presented in fig. 6.24 and fig. 6.26, it's possible to view that high frequencies produce larger variations in contact force magnitude. The robust controllers and *PID* proved to be inefficient for frequencies of up to $20Hz$, when maintaining the $2Hz$ configuration parameters. In real applications the controller has to withstand step and sine type perturbations. The main conclusion is that for these model conditions, no controller developed proved to be efficient in force attenuation for perturbation frequencies of $20Hz$. An experiment done for a $2Hz$ sine frequency with robust controllers, was to lower the robustness bound, thus turning the system closer to the instability limit. Nonetheless, here was found a remarkable performance, when comparing to the previous robust

controller; the downfall of this is that the step response got more oscillatory, and thus the robust margin reduced.

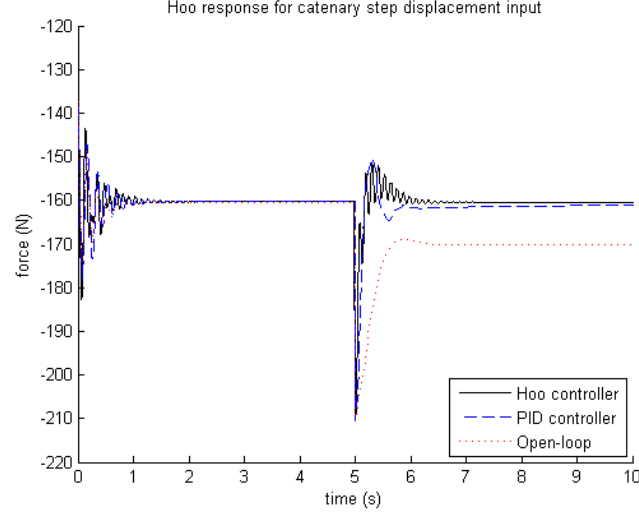


Figure 6.25: Type 1 step perturbation with new controller

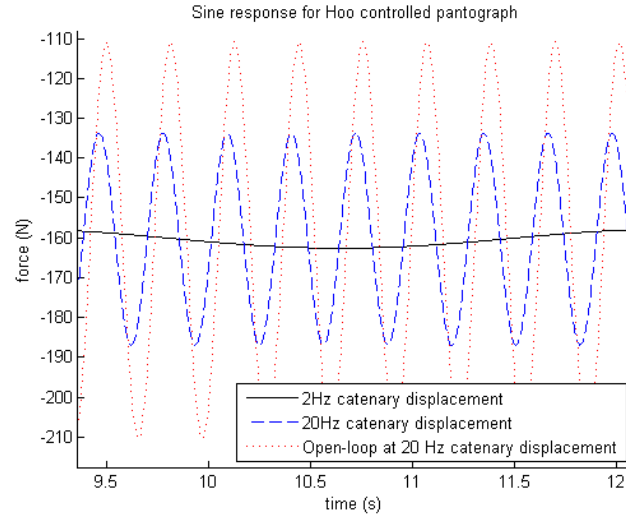


Figure 6.26: Type 1 with 20Hz sine perturbation and new controller

The new configurations set uses slightly different weighting function as presented next:

$$w_1 = \left(\frac{w_0}{\tau s + 1}\right)^n, w_2 = 0.1, w_3 = 10^{-6} \quad (6.14)$$

$$w_0 = 50; \tau = 50; n = 1 \quad (6.15)$$

Although relaxing the w_3 actuator effort weighting function which gives us easier convergence in the

6.8 Closed-loop pantograph analysis

minimization process, it also creates more unstable parameter because the relaxation means that the performance/robustness criteria will also be relaxed. And thus the solutions may have better performance but is less robust to model variations.

The new H_∞ controller is defined by:

$$A = \begin{bmatrix} -1.245 & 6.585 & 7.985 & 1.026 & 7.993 & -1.336 \\ -1.408 & 7.447 & 9.031 & 1.16 & 9.039 & -1.511 \\ 3.244 & -1.716 & -2.08 & -2.672 & -2.082 & 3.481 \\ -6.813 & 3.603 & 4.369 & 5.613 & 4.373 & -7.31 \\ 4.5e & -2.38 & -2.886 & -3.707 & -2.888 & 4.828 \\ -5.54 & 2.93 & 3.552 & 4.564 & 3.556 & -5.944 \end{bmatrix} \quad (6.16)$$

$$B = \begin{bmatrix} -0.02537 \\ 0.06936 \\ 0.03229 \\ 0.05437 \\ 0.05376 \\ -0.05482 \end{bmatrix} \quad (6.17)$$

$$C = \begin{bmatrix} -6.357 & 3.362 & 4.077 & 5.237 & 4.081 \end{bmatrix} \quad (6.18)$$

$$D = \begin{bmatrix} 0 \end{bmatrix} \quad (6.19)$$

For a first approach, one could think that there isn't any better way to improve results with the controllers used, specially knowing that there are more complex models like the Type 3 model. This particular model is considerably more complex, in the way the catenary relates with the pantograph registration strip frame, when compared with the Type 1 model. To better understand the problem it's important to understand that using a step function as perturbation isn't sufficient for controller validation because of the model dynamics and because the experimental data used has a periodic shape. At this point we have two options: the first is to use a square input perturbation wave which would be the hardest control test it's an extension of a step function which excites all system frequencies; the second is a high frequency sine wave, for simplicity reasons and to better resemble

the actual catenary effect, a sine wave was chosen, thus from here on, this study will try to solve the sine perturbation control problem maintaining the quality of the step response (always checking the step response). The closed-loop response for a sine perturbation with the same properties as previous sine tests for the Type 3 model are presented in fig. 6.27 and fig. 6.28.

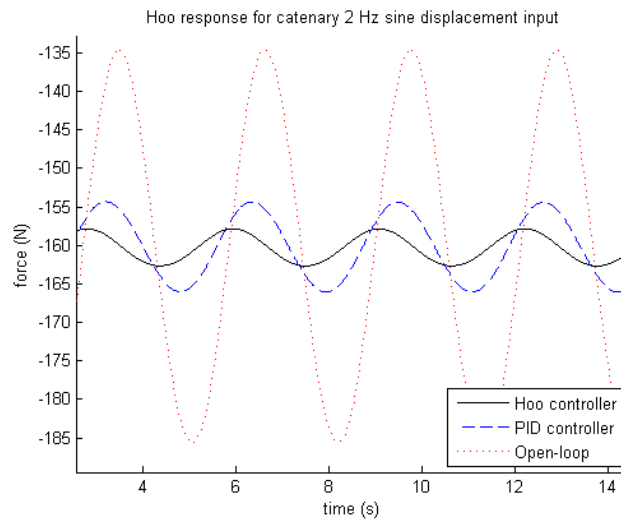


Figure 6.27: Type 3 with 2Hz sine perturbation with new controller

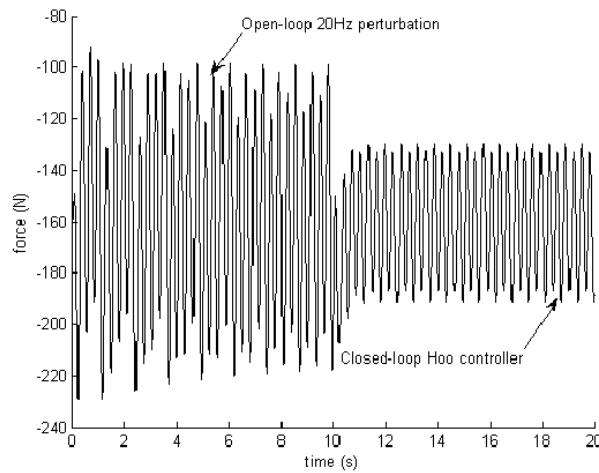


Figure 6.28: Type 3 with 20Hz sine perturbation and new controller

The registration strip in the Type 3 model is more complex than the standard 1 *DOF* vertical registration strip defined by the Type 1 model. This model (the Type 3) has 1 rotation *DOF* and 1 translation *DOF*, and to further approximate the *SimMechanics*[®] model to a real pantograph

6.8 Closed-loop pantograph analysis

implementation, the motion of the catenary along the registration strip frame is considered. In this context, the same controller developed for the Type 1 model was used for the Type 3 model and the results for high frequencies were as expected: they were very poor. These results and this conclusion comes from an extensive trial and error weight function development.

At this point, it was thought that it was a very complicated task to control high frequencies in the contact interface of the pantograph. From all the studies made till now, no modifications to the models were made, with one exclusion which is in section 5. Because the catenary already contains a damper, problems were found due to the existence of instant catenary movement (like the step perturbation), which caused an infinite force magnitude. This happened because we considered that the catenary displacement was infinity fast, thus moving instantly to the final step position. Because $F_c = C(dx/dt - dx_0/dt)$ and because for a step $\Delta T = 0$, $dx/dt = \infty$, means that the force tends to infinity. Because the numeric integrator has its own step time, the system doesn't crash, but this "glitch" explains why the controller didn't have good performance in the first place, for high frequency solicitations on the pantograph. In the step response with the same Type 3 model, the damper has a good energy absorption, but if we introduce a controller to this joint, letting the passive damper element there, the controller effectiveness is largely reduced. In contrast, the spring only intensifies the energy cost to move the joint. Because energy optimization isn't the main focus in this work, the springs are maintained, but the dampers are eliminated in the actuated joints. These modifications improves the performance of the robust and *PID* controllers in every actuated joint for every model. In fig. 6.29 it's possible to see the improvement in control, due to the changes made in the model for an H_∞ controller for a Type 1 and a Type 3 model. The only problem of this is when there is no control and because this situation can occur in real pantograph circulation this can be a big problem. Removing the lower damper can turn the open loop response more oscillatory.

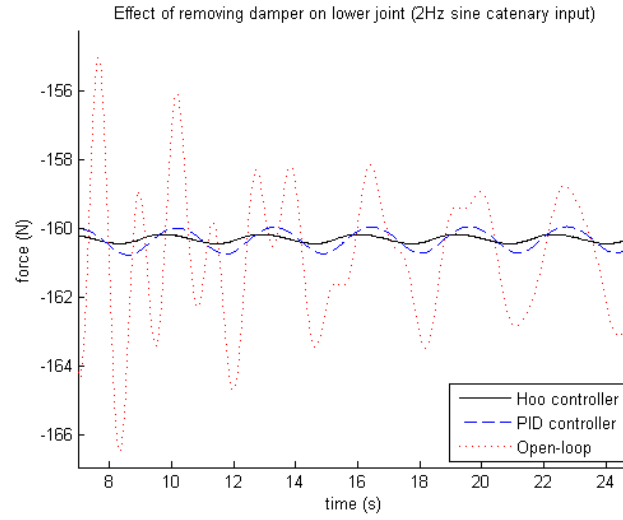


Figure 6.29: H_∞ controller, with no damper in lower joint

The controller used is the same for both. And as can be seen from the figures presented, the results are better than the previous. A lesson can be learned from this experiment which is that many times, if possible, the model has to be optimized for control. Not including passive elements in the pantograph lower joint, doesn't constitute any problem, and as the results show it makes great difference. These results can be extended to pneumatic cushions, which act in a certain way as a damper and thus from the results, it would be interesting to compare cushion actuated joints with electrical motor joints, passing for control the spring and damping effects. Still for real circulation for robust implementation reasons and safety, the inclusion of some sort of damping would be important, enough to absorb some train and pantograph element dynamics but not so much to constitute a controller restrainer.

6.9 Mixed control analysis

Until this point, only one actuated joint was considered. Here, we will consider two actuator Joint. One between the base and the lower arm joint, and another one between the stabilization arm and registration strip. The upper actuator is represented by two actuators, but because the motion of this

6.9 Mixed control analysis

joint is a vertical 1 *DOF* movement, and because the model considered is of a Type 4 model, it's as if only one actuator existed and was applied to the center. An important test that is illustrated in fig 6.30, and fig. 6.31 are model responses to several types of perturbations: with one actuated joint on the lower arm; with one actuated joint on the registration strip; or both actuated joints separately.

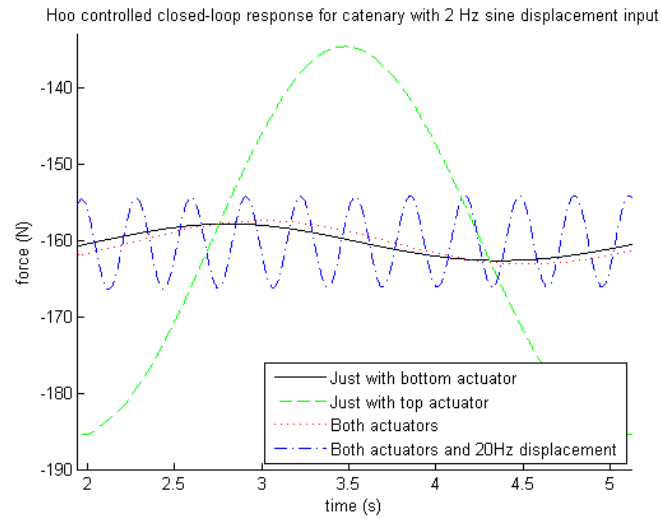


Figure 6.30: Type 4 controller implementation results to sine perturbation

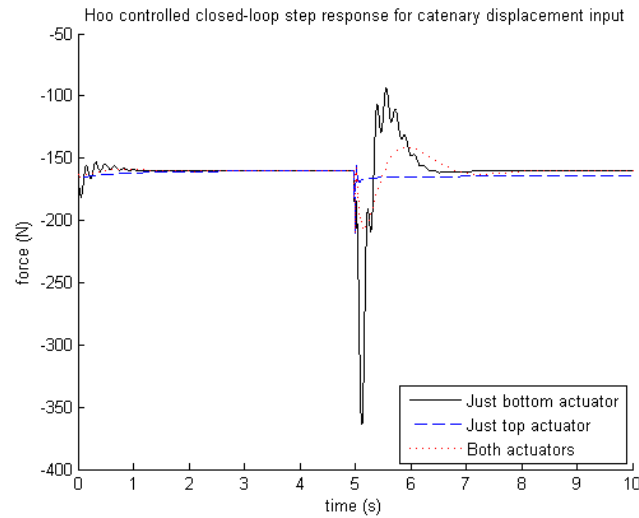


Figure 6.31: Type 4 controller implementation results to step perturbation

It is evident from the figures presented that the use of both controllers improves overall performance, the lower actuated joint absorbs low frequencies and deals with bigger catenary displacements,

and the upper actuated joint deals with higher frequencies. Still it wasn't possible to eliminate the oscillation. The step-perturbed system continues to give good results for controllers.

6.10 Sliding catenary control

The Type 5 model follows the same theory and assumptions of the Type 4 model, but this time the model is actuated on both joints.

The sliding mode controller developed is based on simple information of catenary position along the registration strip frame. This means that the control power varies with cable position along the way. The controllers were tested separately in fig. 6.32 and in conjunction in fig. 6.33 for a catenary frequency input of $2Hz$.

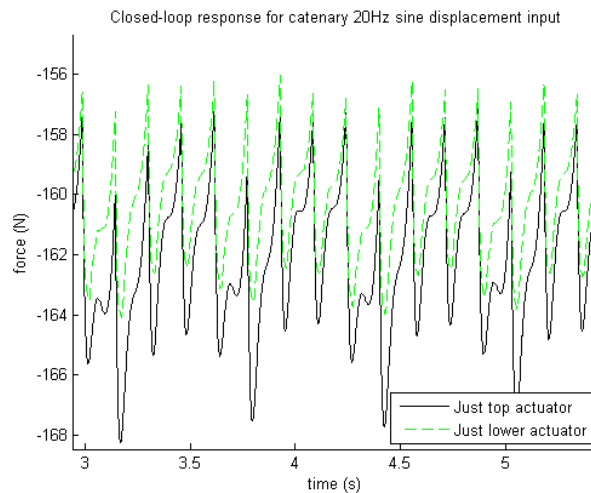


Figure 6.32: Independent control function of Type 5 model

The objective in this section is to have three inputs controlled separately with the same control objective. Because the catenary slides along the frame and because we have to upper controllers in the registration strip, one in the left and the other in the right. There will be times where the cable will be totally on the left or the right, this means that not always will be a good idea for the actuator

6.11 Controller robustness to model changes

to follow the reference. In summary the controller power is affected by the catenary motion, thus maximum when the cable is on top of the actuator and minimum when at the most distant point.

The results can be seen in fig. 6.33 for a catenary frequency input of $2Hz$.

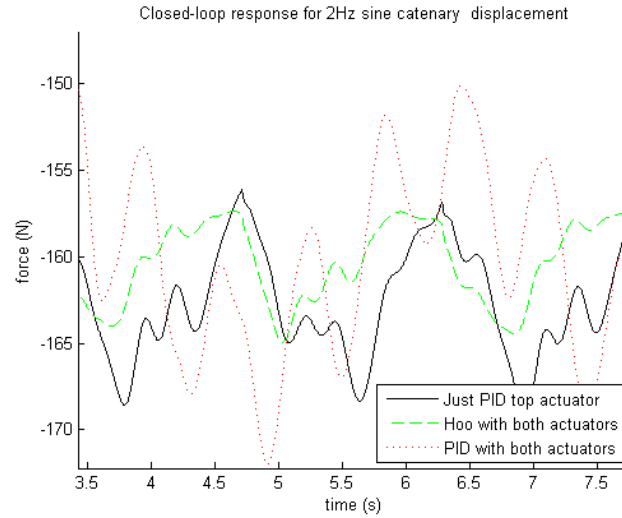


Figure 6.33: Type 5 control implementation for $2Hz$ perturbation

6.11 Controller robustness to model changes

Although in previous sections model robustness was tested, in this particular section the differences between robust and *PID* controllers are put to evidence. One can verify big difference in robust control if we change some critical element in the machine presented. If the controller were to be robust the performance bound will contain the expected frequency range variation which results from perturbations in the system or modelling errors. Many tests were made like adding white noise to the signal or simply by changing model attributes.

To show how a model parameter can shift the natural frequencies of the system, the damper element present in the lower arm was removed, the results can be viewed in fig. 6.34, the model in study is the Type 1 model.

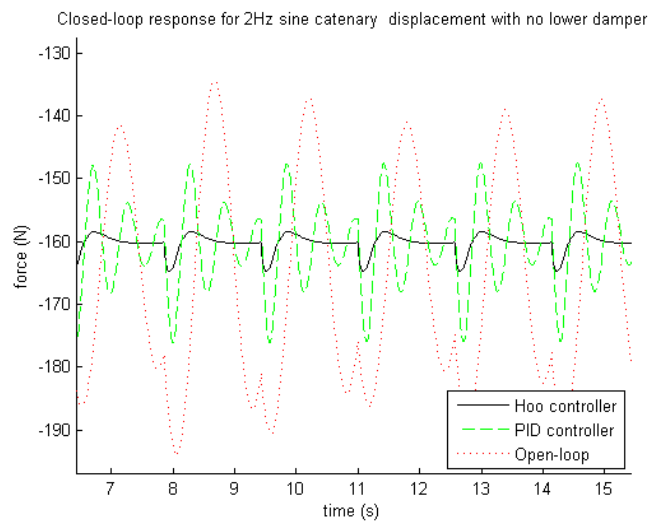


Figure 6.34: H_∞ VS PID controlled with altered model (no lower damper)

As can be seen from fig. 6.34 the PID which worked in normal conditions doesn't work in the new ones. The robust controller adapted well to this perturbation signal because it was developed to work in a frequency range of 2 to 20 Hz. This modelling desire can be bad for example in a step that excites all frequencies meaning that the controller can have poor results here. To test the controllers, white noise was introduced in the Type 5 model and the results presented in fig. 6.35. From fig. 6.35 it's possible to see that the output noise influences the signal greatly. The noise added was exaggerated to see which of the controllers could withstand such condition. What can be seen is that the robust controller is more insensible to noise compared with a PID controller.

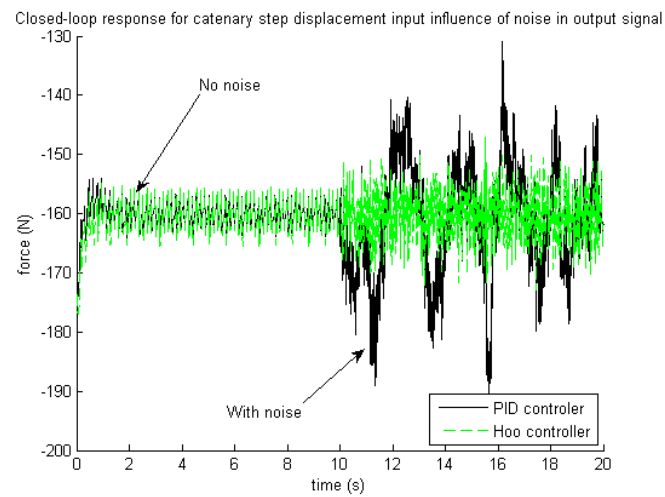


Figure 6.35: Noise influence on Type 1 model with 2Hz catenary influence

Chapter 7

Conclusions and future work

The main objective of this project was to design and control a pantograph, with robust stability. To engage these objectives a pantograph model was created. The model presented in this study isn't the exact model used by the *SNCF* pantograph, it's a mere simplification of the real model.

In this work it wasn't only intended to study a pantograph for high speeds but to study the feasibility of using in standard train speed lines, controlled pantograph. The inclusion of control in pantograph systems cannot only be associated to decreasing the travel time between destinations, it has a more broader area of influence. Pantograph systems have typically low maintenance, but this machine is an expensive component of the train, due to its robustness to sustain physical contact with the wires and to resist to bad weather conditions and electric arc formations. Traditional approaches (with no control) resort to aerodynamic wings in the registration strip. Good results have been obtained resorting to this technology using the air lift that rises the registration strip with higher train velocities ensuring better contact at high speeds. But excessive wear to the interface elements still occur and pantograph fixation to the cable system are still present. Evolving to systems that have very low wear to the pantograph and catenary, that have very low maintenance and have minimum risk

of pantograph fixation to the cable system are a very appealing solution for every train transportation company.

It was shown, for the models Type 1 and Type 2, that these are simple and easy to linearize and control. Compared to the Type 3 model. Robust stability was obtained for H_2 and H_∞ controllers (following [8] and [9]), and proved that modifying these models in reasonable values, the controller still reaches reasonable margins of stability providing acceptable results. Acceptable results are better results than the ones provided by the experimental data thus the force amplitude being the lower as possible.

Regarding to modelling, it was shown that standard one dimensional registration strip, doesn't model exactly the real dynamics of a pantograph due to catenary movement along the registration strip. The model that was found to represent better the real system was the Type 3 model. The Type 1 and the Type 3 models don't approximate correctly the experimental results in amplitude and in frequency because they weren't projected with the experimental results. Furthermore it is important to reconstruct the model based on the target experimental model frequencies and amplitudes.

Finding the right sensitivity transfer functions was a wearisome ordeal, because the working frequencies of a pantograph can go up to 20 Hz (20 Hz of perturbation signal). Providing a controller that could be robust and have good performance, wasn't possible for the Type 3 model, so a compromise had to be reached.

From the experiments made in control it was found that high input frequencies applied on the pantograph affect the control performance, this means that the controller must only work in specific frequency regions for safety reasons.

Lower arm damper effect was studied and found to be a critical element in high frequencies with high amplitudes. Although a damper limits the actuated inputs on how fast it responds to system change, it is a instant energy absorber and therefore a better it is important to have a better combination of damper and actuator constant values for better controlling. Upper active elements proved to be efficient with low amplitude high frequencies.

In general, the robust controller proved to be better than a normal *PID* controller with exception to the tuning steps which are more complex. It's not elementary to find the right combination of weights that filter the objective designer frequency specifications for the robust controllers. Further more as expected the robust controller proved to have better performance to model parameter changes and signal noise than the *PID* controller.

7.1 Future work

Using a standard train pantograph would be the ideal experimental platform for more results and comparisons. In this work a *SimMechanics*[®] model was developed, with this we can now compare with other types of approaches, moreover a model like the Type 1 but built upon the closed chains *Denavit-Hartenberg* method. The objective is to have a more numerically efficient method for realtime applications. This could be useful for system observers or real time animations. The method suggested is different than the standard global coordinates approaches, having good potentialities due to it's simplicity comparing to other approaches.

Bibliography

- [1] B. Allotta, M. Papi, P. Toni, and A. G. Violi. Experimental campaign on a servo-actuated pantograph. *Advanced Intelligent Mechatronics*, 1:237–242, 2001.
- [2] Park Tong Jin, Han Chang Soo, and Jang Jin Hee. Dynamic sensitivity analysis for the pantograph of a high-speed rail vehicle. *Journal of Sound and Vibration*, 266:235–260, 2002.
- [3] Jong-Hwi Seo, Seok-Won Kim, Il-Ho Jung, Tae-Won Park, Jin-Yong Mok, Young-Guk Kim, and Jang-Bom Chai. Dynamic analysis of a pantograph - catenary system using absolute nodal coordinates. *Elsevier*, 44:615–630, 2006.
- [4] M. Schaub. and B. Simeon. Pantograph - catenary dynamics: An analysis of models and simulation techniques. *Mathematical and Computer Modelling of Dynamical Systems*, Vol. 7:225–238, 2001.
- [5] A. Kumaniecka. Dynamics of an overhead line and pantograph system. *The Dynamics of vehicles on roads and on tracks*, pages 104–113, 1998.
- [6] W. M. Zhai and C. B. Cai. Effect of locomotive vibrations on pantograph-catenary system dynamics. *The dynamics of vehicles on roads and on tracks*, 29:47–58, 2000.
- [7] A. Pisano and E. Usai. Output-feedback regulation of the contact-force in high-speed train pantographs. *Dynamic Systems, Measurement, and Control*, 126:82–87, 2004.

BIBLIOGRAPHY

- [8] A. Collina, A. Facchinetti, F. Fossati, and F. Resta. An application of active control to the collector of an high-speed pantograph: Simulation and laboratory tests. *Advanced Intelligent Mechatronics, 2001. Proceedings. 2001 IEEE/ASME International Conference*, 1:243–248, 2005.
- [9] D. J. Hartland. Developments towards an active pantograph. *Current Collections for High Speed Trains Seminar (Ref. No. 1998/509)*, IEE, Current Collections for High Speed Trains Seminar: 5/1–5/5, 1998.
- [10] J. Y. S. Luh and Yuan Fang Zheng. Computation of input generalized forces for robots with closed kinematic chain mechanisms. *Robotics and Automation, IEEE Journal of [legacy, pre - 1988]*, pages 95– 103, 1985.
- [11] Xiang-Rong Xu, Won-Jee Chung, Young-Hyu Choi, , and Xiang-Feng Ma. A new dynamic formulation for robot manipulators containing closed kinematic chains. *Robotica*, 17:261–267, 1999.
- [12] Giles D. Wood and Dallas C. Kennedy. Simulating mechanical systems in simulink with simmechanics. *The Mathworks, Inc., www.mathworks.com/matlabcentral/fileexchange/(PDF file)*, MA, USA, 2003.
- [13] Leon Žlajpah. Simulation of robotic manipulators. *RAAD 2006*, 2005.
- [14] F. Kiessling, W. Harprecht, and R. Seifert. Tractive power supply at german federal railway’s 400 km/h runs. *Railroad Conference, 1989. Proceedings., Technical Papers Presented at the 1989 IEEE/ASME Joint*, pages 23–32, 1989.
- [15] Faiveley. *CX - The piloted pantograph system for optimal current collection*. Faiveley Transport, 2006.

- [16] The Mathworks. *The MathWorks, Inc. SimMechanics Users Guide*. The MathWorks, November 2002.
- [17] D. Pai, U. Ascher, and P. Kry. Forward dynamics algorithms for multibody chains and contact. *IEEE International Conference on Robotics and Automation*, 2:857–863, 2000.
- [18] Uri M. Ascher, Dinesh K. Pai, , and Benoit P. Cloutier. Forward dynamics. elimination methods, and formulation stiffness in robot simulation. *Technical report, Department of Computer Science, University of British Columbia*, 1996.
- [19] Ahmed A. Shabana. *Computational Dynamics*. Wiley-Interscience, 2005.
- [20] P. C. Chandrasekharan. *Robust Control of Linear Dynamical Systems*. Academic Press, 1996.
- [21] M. C. Close and D. K. Frederick. *Modeling and Analysis of Dynamic Systems*. Houghton Mifflin Company, 1974.
- [22] J. Ackermann. *Robust Control, Systems with Uncertain Physical Parameters*. Springer-Verlag, 1993.
- [23] Miguel Ayala Botto. *Controlo de Sistemas, acetatos das aulas teóricas*. Departamento de Engenharia Mecânica, Secção de sistemas, 2006.
- [24] Sigurd Skogestad and Ian Postlethwaite. *Multivariable Feedback Control - Analysis and Design*. John Wiley & Sons, 2005.
- [25] Kemin Zhou, John Doyle, and Keith Glover. *Robust and Optimal control*. Prentice Hall, 1996.
- [26] Miguel Ayala Botto. *Controlo Não Linear, acetatos das aulas teóricas*. DEM, 2004.
- [27] The Mathworks. *Control System Toolbox 8 User's Guide*. The Mathworks, 2007.

BIBLIOGRAPHY

- [28] J. P. Menuet. *Training Session in High Speed Systems*. SNCF, 2006.
- [29] Gary Balas, Richard Chiang, Andy Packard, and Michael Safonov. *Robust Control Toolbox*. The Mathworks, The MathWorks, Inc. 3 Apple Hill Drive Natick, MA 01760-2098, 2006. Users Guide.
- [30] D. Abramovitch. "some crisp thoughts on fuzzy logic", proceedings of the american control. *Proceedings of the American Control Conference*,, pages 168–172, 1994.
- [31] Uri M. Ascher, Hongsheng Chin, Linda R. Petzold, and Sebastian Reich. Stabilization of constrained mechanical systems with daes and invariant manifolds. *Technical report, Department of Computer Science*, 1994.
- [32] J. K. Astrom. Adaptive control around 1960. *IEEE Control Systems*, 1:44–49, 1996.
- [33] Aldo Balestrino, Ottorino Bruno, Alberto Landi, and Luca Sani. Innovative solutions for overhead catenary-pantograph system wire actuated control and observed contact force. *Vehicle System Dynamics*, 33:69–89, 2000.
- [34] Claus Bendtsen and Per Grove Thomsen. *Numerical Solution of Differential Algebraic Equations*. Department of Mathematical Modelling, Technical University of Denmark, 1999.
- [35] Robert H. Bishop. *Modern Control Systems Analysis and Design Using Matlab*. Addison-Wesley, 2005.
- [36] Miguel Ayala Botto. *Identificação de Sistemas, acetatos das aulas teóricas*. Departamento de Engenharia Mecânica, Secção de sistemas, 2003.
- [37] W. P. Boyle and K. Liu. The fourbar linkage pseudographic kinematic analysis. *Int. J. Engng Ed.*, 13:262–268, 1997.
- [38] Roland S. Burns. *Advanced Control Engineering*. Butterworth-Heinemann, 2001.

- [39] Union Internationale des Chemins de fer. *Code UIC 505-1*. Union Internationale des Chemins de fer, 1997.
- [40] Union Internationale des Chemins de fer. *Code UIC 505-5*. Union Internationale des Chemins de fer, 1997.
- [41] Peter I. Corke. *Robotics Toolbox*. CSIRO, 2002.
- [42] Ad Damen and Siep Weiland. Robust control.
- [43] Roy Featherstone and David Orin. Robot dynamics: Equations and algorithms. *Robotics and Automation, 2000. Proceedings. ICRA '00. IEEE International Conference*, 1:826–834, 2000.
- [44] Luc Jaulin, Michel kieffer, Olivier Didrit, and Eric Walter. *Applied Interval Analysis With Examples to Parameter and State Estimation Robust Control and Robotics*. Springer, 2001.
- [45] Ogata Katsuhiko. *Modern Control Engineering, Third edition*. Longman Pearson Education, 1997.
- [46] Haniph A. Latchman. *Simulink Control Design 2 User's guide*. Matlab, 2007.
- [47] Haniph A. Latchman. *Modern Control Systems - A State Variables Approach*. University of Florida, Electrical & Computer Engineering, 2003.
- [48] Michael Lemmon. *Robust Control Multivariable Control*. Dept. of Electrical Engineering, University of Notre Dame, 2005.
- [49] Michael Lemmon. *Essentials of Robust Control*. Dept. of Electrical Engineering, University of Notre Dame, 2005.
- [50] Daniel R. Lewin. *Process Control Laboratory*. Department of Chemical Engineering, 2003.

BIBLIOGRAPHY

- [51] F. L. Lewis. *Optimal Estimation with an Introduction to Stochastic Control Theory*. John Wiley & Sons, 1986.
- [52] Jorge M. M. Martins. *Modelling and identification of flexible manipulators towards robust control*. Tese de Mestrado, Universidade Tcnica de Lisboa, Instituto Superior Técnico, Portugal, 2000.
- [53] Parviz E. Nikravesh. *Computer-Aided Analysis of Mechanical Systems*. Prentice Hall, 1987.
- [54] Z. Qu. *Robust Control of Nonlinear Uncertain Systems*. John Wiley & Sons, 1998.
- [55] Ricardo S. Sanchez-Pena and Mario Sznaiier. *Robust Systems, theory and applications*. John Wiley & Sons, 1998.
- [56] Paula Silva, Relógio Ribeiro, and Nuno Maia. *Vibrações e Ruído - Guia de ensaios experimentais*. Secção de projecto mecânico, edição aeist edition, 2001.
- [57] Mark W. Spong and M. Vidyasagar. *Robot Dynamics and Control*. Jonh Wiley & Sons, 1989.
- [58] Chia-Chi Tsui. *Robust Control System Design Advanced State Space Techniques*. Marcel Dekker, 2004.